Scuola di Dottorato Leonardo da Vinci – a.a. 2010/11

LASER: CARATTERISTICHE, PRINCIPI FISICI, APPLICAZIONI

Versione 3 – Dicembre 11 – http://www.df.unipi.it/~fuso/dida

Parte 7
Proprietà della luce laser e sue caratteristiche per impieghi metrologici

Me 07.12.11 16-18 aula DIC
Me 14.12.11 16-17 aula DIC
Ve 16.12.11 16-18 aula DIC

SOMMARIO

Sappiamo che la luce laser ha proprietà uniche (monocromaticità, coerenza, brillanza, etc.) e sappiamo come è fatto un laser

- Proprietà della luce laser e strategie di miglioramento:
  - monocromaticità
  - coerenza temporale e spaziale
  - brillanza

- Applicazioni che sfruttano direttamente le caratteristiche della luce laser:
metrologia (in solidi e plasmi)

Obiettivo : capire l'origine delle proprietà del laser

Obiettivo: verificare l'importanza delle caratteristiche della luce laser in applicazioni specifiche di alto interesse tecnologico, e.g., misure e caratterizzazioni

MONOCROMATICITÀ

1.4. PROPERTIES OF LASER BEAMS

Laser radiation is characterized by an extremely high degree of monochromaticity, coherence, directionality, and brightness. We can add a fifth property, viz., short duration, which refers to the capability of producing very short light pulses, a less fundamental but nevertheless very important property. We now consider these properties in some detail.

1.4.1. Monochromaticity

This property is due to the following two circumstances: (1) Only an em wave of frequency ν given by Eq. (1.1.1) can be amplified. (2) Since a two-mirror arrangement forms a resonant cavity, oscillation can occur only at the resonance frequencies of this cavity. The latter circumstance leads to an often much narrower laser linewidth (by as much as 10 orders of magnitude) than the usual linewidth of the transition $2 \rightarrow 1$, as observed in spontaneous emission.

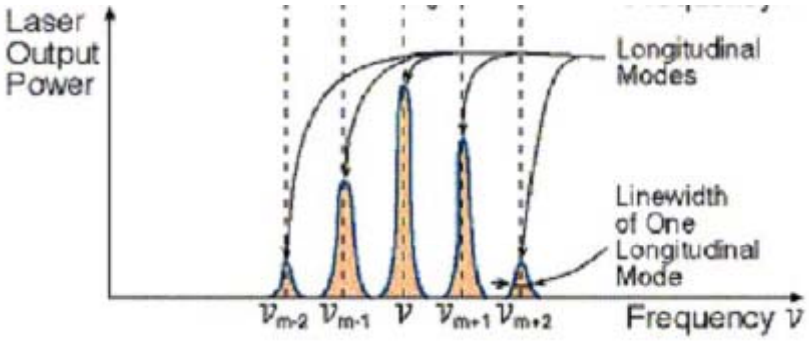

Larghezza di riga del laser regolata (anche) da larghezza di riga della cavità

Il carattere monocromatico dipende da:
- Selezione singolo modo longitudinale;
- Larghezza del modo (cavità);
- (spesso) selezione modo trasversale

Avevamo definito: $Q = 2\pi c/(\alpha\lambda) = \omega/\alpha = \omega\tau$
τ: vita media fotone in cavità

Andamento temporale campo e.m. nella cavità: $E(t) = E_0 e^{-i\omega t} e^{-\alpha t}$

Componente Fourier a pulsazione Ω:

$$\tilde{E}(\Omega) \propto \int_0^\infty E(t) e^{i\Omega t} dt = E_0 \int_0^\infty e^{i(\Omega - \omega + i\alpha)t} dt \propto \frac{E_0}{i\left[(\Omega - \omega) + i\alpha\right]}$$

Densità energia e.m. (ovvero potenza):

$$u(\Omega) \propto |\tilde{E}(\Omega)|^2 = \frac{|E_0|^2}{\left[(\Omega - \omega)^2 + \alpha^2\right]}$$

Larghezza di riga della cavità: $\Delta\omega_{cavità} \propto \alpha = \frac{\omega}{Q}$

STRATEGIE DI AUMENTO *Q*

Intracavity etalon

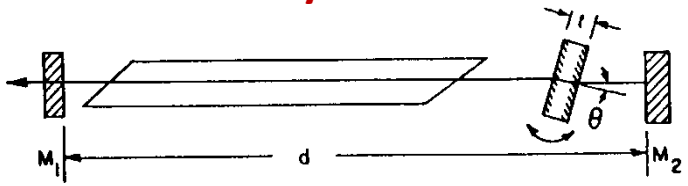

Fig.5.36. Single-mode operation by inserting a tilted etalon inside the laser resonator

In optics, a **Fabry-Pérot interferometer** or **etalon** is typically made of a transparent plate with two reflecting surfaces, or two parallel highly reflecting mirrors. (Technically the former is an etalon and the latter is an interferometer, but the terminology is often used inconsistently.) Its transmission spectrum as a function of wavelength exhibits peaks of large transmission corresponding to resonances of the etalon. It is named after Charles Fabry and Alfred Perot.[1] "Etalon" is from the French *étalon*, meaning "measuring gauge" or "standard".[2]

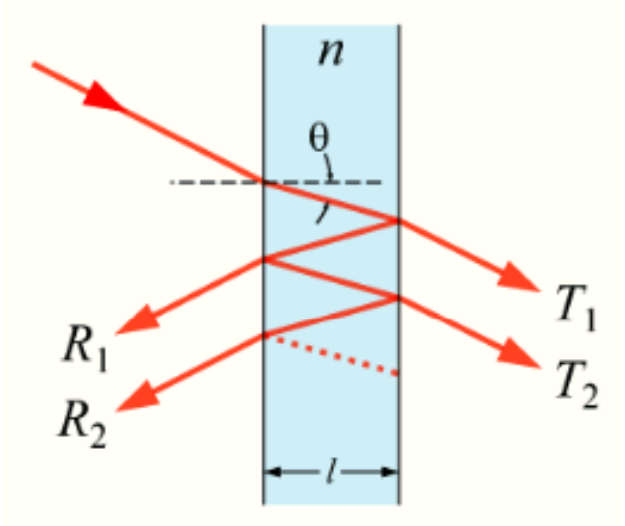

A Fabry-Pérot etalon. Light enters the etalon and undergoes multiple internal reflections.

The phase difference between each succeeding reflection is given by δ:

$$\delta = \left(\frac{2\pi}{\lambda}\right) 2nl\cos\theta.$$

f.s.r. etalon: $\delta = m\pi$

If both surfaces have a reflectance R, the transmittance function of the etalon is given by:

$$T_e = \frac{(1-R)^2}{1+R^2-2R\cos(\delta)} = \frac{1}{1+F\sin^2\left(\frac{\delta}{2}\right)}$$

where $F = \frac{4R}{(1-R)^2}$ is the *coefficient of finesse*.

Finezza dell'etalon

The varying transmission function of an etalon is caused by interference between the multiple reflections of light between the two reflecting surfaces. Constructive interference occurs if the transmitted beams are in phase, and this corresponds to a high-transmission peak of the etalon. If the transmitted beams are out-of-phase, destructive interference occurs and this corresponds to a transmission minimum. Whether the multiply-reflected beams are in-phase or not depends on the wavelength (λ) of the light (in vacuum), the angle the light travels through the etalon (θ), the thickness of the etalon (l) and the refractive index of the material between the reflecting surfaces (n).

FINEZZA E LARGHEZZA DI RIGA

$$T_e = \frac{(1-R)^2}{1+R^2-2R\cos(\delta)} = \frac{1}{1+F\sin^2(\frac{\delta}{2})}$$

where $F = \frac{4R}{(1-R)^2}$ is the *coefficient of finesse*.

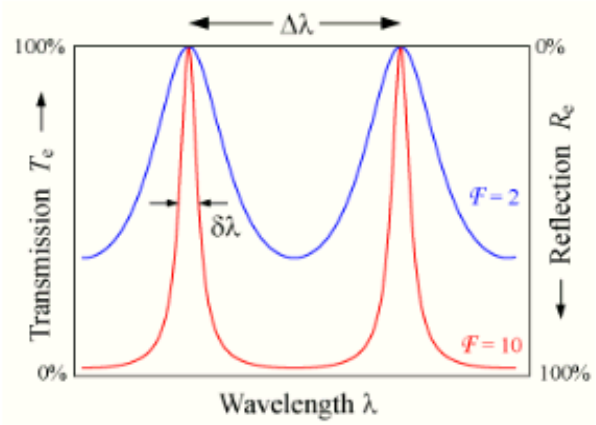

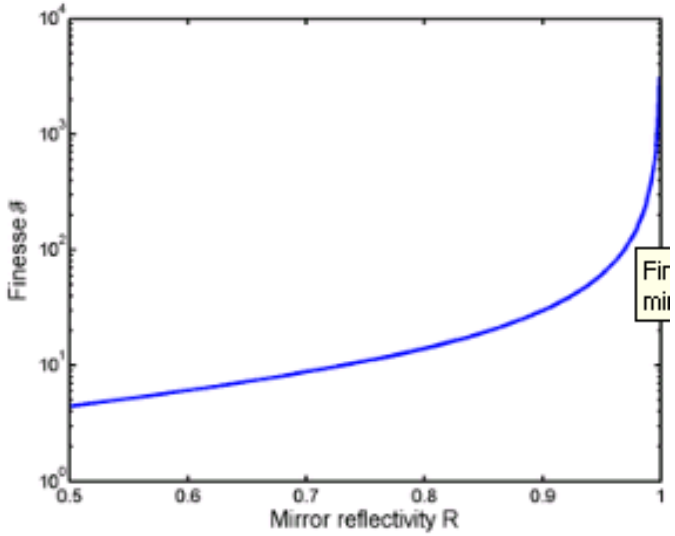

Possibile realizzare etalon con finezza > 10^3
(a scapito della trasmissione media, cioè
fuori dai modi consentiti)

Larghezze di riga *tipiche* per laser CW (in continua):

- Laser a gas (HeNe, Ar^+,…): $\Delta\nu < 1$ MHz (anche < 1 kHz per laser con cavità ultrastabili)
- Laser a stato solido (Nd:YAG, TiSa, centri di colore, …): $\Delta\nu \sim 1$ MHz (anche < 10 kHz con etalon)
- Laser a colorante: $\Delta\nu \sim 100$ MHz (fino a 100 kHz per laser con etalon)
- Laser a diodo: $\Delta\nu \sim 1$ MHz (anche < 10 kHz per laser con cavità esterna)

Attenzione: drift termico e jitter introducono fluttuazioni a tempi “lunghi”!

LIMITE QUANTISTICO

Schawlow–Townes Linewidth

Definition: linewidth of a single-frequency laser with quantum noise only

Even before the first laser was experimentally demonstrated, Schawlow and Townes calculated the fundamental (quantum) limit for the linewidth of a laser [1]. This lead to the famous *Schawlow–Townes equation*:

Esiste limite quantistico per larghezza di riga dovuto a fluttuazioni quantistiche (em. spont.)

$$\Delta\nu_{\text{laser}} = \frac{\pi h\nu \left(\Delta\nu_c\right)^2}{P_{\text{out}}}$$

Es.: HeNe, $h\nu$=2eV, $\Delta\nu_C$=1MHz, P_{out}=1mW → $\Delta\nu_{S.T.}$~1mHz!!

with the photon energy $h\nu$, the resonator bandwidth $\Delta\nu_c$ (full width at half-maximum, FWHM), and the output power P_{out}. It has been assumed that there are no parasitic cavity losses. (Compared with the original equation, a factor 4 has been removed because of a different definition of the resonator bandwidth.)

It is often claimed that the phase noise level corresponding to the Schawlow–Townes linewidth is a result of spontaneous emission into the laser mode. Although this picture is intuitive, it is not completely correct. Both the laser gain and the linear losses of the laser resonator contribute equal amounts of quantum noise to the intracavity light field. This means that even when replacing laser gain with some noiseless amplification process, the phase noise would only decrease to half of the Schawlow–Townes value [2].

Carefully constructed solid-state lasers can have very small linewidths in the region of a few kilohertz, which is still significantly above their Schawlow–Townes limit: technical excess noise makes it difficult to reach that limit. The linewidth of semiconductor lasers is also normally much larger than according to the original equation (without the α factor). This, however, is largely caused by amplitude-to-phase coupling effects (which can be quantified with the linewidth enhancement factor), and not by technical excess noise.

Altre fluttuazioni “tecnologiche” (es. fase/ampiezza) generalmente più importanti di limite Schawlow-Townes

PROPRIETÀ LUCE LASER

Già annunciate:
- *Monocromaticità*
- Coerenza (spaziale e temporale)

Non ancora introdotte:
- [Brillanza (intensità e collimazione/focalizzazione)]

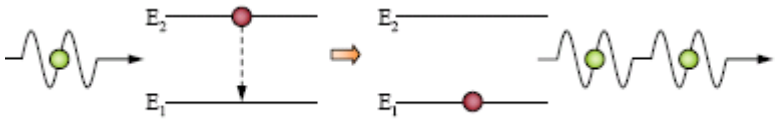

EMISSIONE COERENTE

DUE FOTONI INDISTINGUIBILI: STESSA FREQUENZA, DIREZIONE, FASE E POLARIZZAZIONE

In termini semplici possiamo pensare ad una sorta di "ordine" dei fotoni

In pratica una coerenza elevata implica una elevata focalizzabilità del laser (macchia focale molto piccola, intensità elevata)

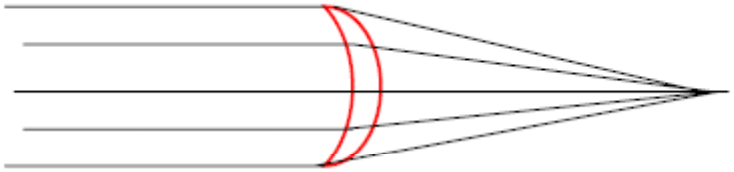

INTERFEROMETRIA

The principle of superposition of waves states that when two or more waves are incident on the same point, the total displacement at that point is equal to the vector sum of the displacements of the individual waves. If a crest of a wave meets a crest of another wave of the same frequency at the same point, then the magnitude of the displacement is the sum of the individual magnitudes – this is constructive interference. If a crest of one wave meets a trough of another wave then the magnitude of the displacements is equal to the difference in the individual magnitudes – this is known as destructive interference.

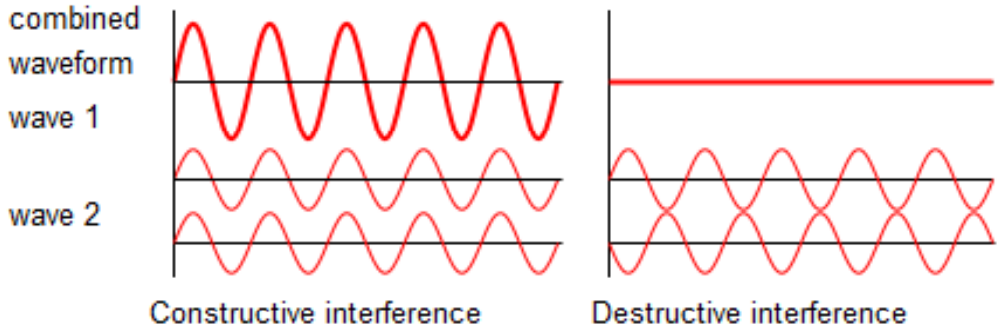

Constructive interference occurs when the phase difference between the waves is a multiple of 2π, whereas destructive interference occurs when the difference is π, 3π, 5π, etc. If the difference between the phases is intermediate between these two extremes, then the magnitude of the displacement of the summed waves lies between the minimum and maximum values.

Interferometro di Michelson

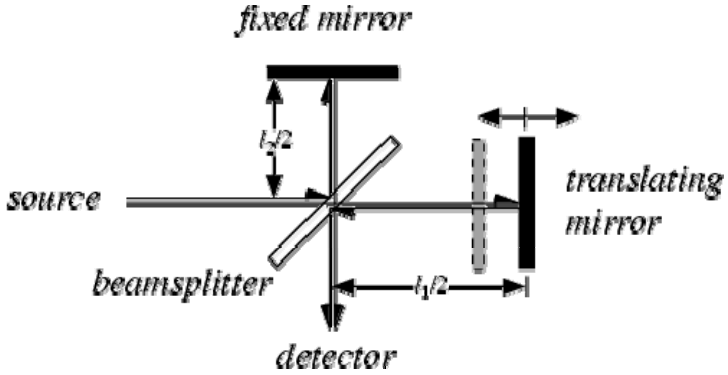

University of Chicago physicist Albert A. Michelson. This year marks the centennial of Michelson's Nobel Prize in Physics. He was the first American to receive a Nobel Prize in the sciences.

INTERFEROGRAMMI DI MICHELSON

Il fascio viene diviso in due e i due fasci fanno percorsi L_1 e L_2

$$\vec{E}_1 = \hat{e}_1 E_1 \exp(i(kL_1 - \omega t))$$
$$\vec{E}_2 = \hat{e}_2 E_2 \exp(i(kL_2 - \omega t))$$

Espressione dei due fasci (onde piane "ideali")

$$\vec{E}_{tot} = \vec{E}_1 + \vec{E}_2 = \exp(i(kL_1 - \omega t))(\hat{e}_1 E_1 + \hat{e}_2 E_2 \exp(ik\Delta L))$$
$$\text{con}: \Delta L = L_2 - L_1$$

Sovrapposizione sul rivelatore

Le polarizzazioni dei due fasci non devono essere ortogonali altrimenti non c'è interferenza
(ill contrasto dipende dal prodotto scalare fra le polarizzazioni)

$$|\vec{E}_{tot}|^2 = |E_1|^2 + |E_2|^2 + (\hat{e}_1 \cdot \hat{e}_2) E_1 E_2 (\exp(ik\Delta L) + \exp(-ik\Delta L)) =$$
$$= |E_1|^2 + |E_2|^2 + (\hat{e}_1 \cdot \hat{e}_2) E_1 E_2 \, 2\cos(k\Delta L)$$

Potenza letta dal rivelatore

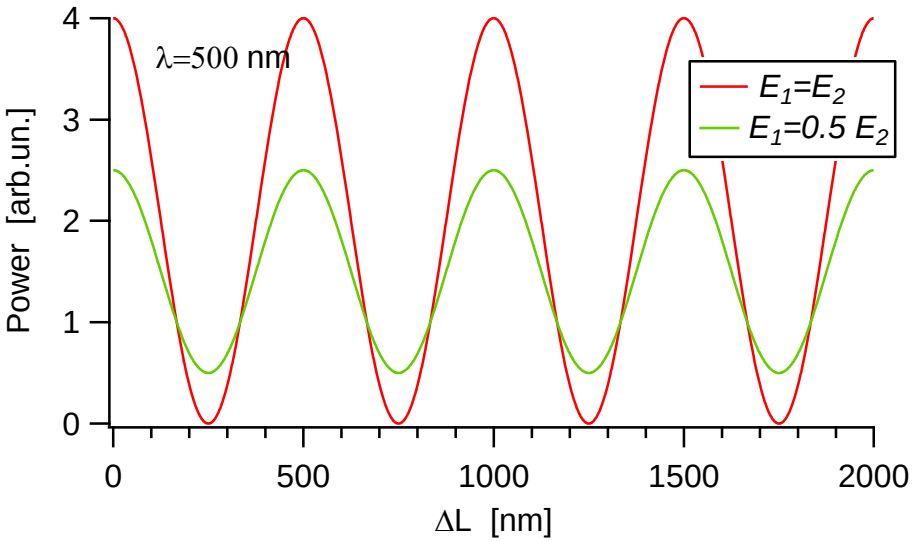

Il segnale (potenza) letto dal rivelatore dipende dalla differenza di cammino (ottico) ΔL

Si può ottenere una grandissima sensibilità (è relativamente facile apprezzare differenze dell'ordine del nm)

FRANGE DI INTERFERENZA

Interference in a Michelson interferometer can be understood in terms of thin-film interference. Imagine that the arms of the interferometer are rotated, such that there is a single optical axis, as shown in the drawing below.

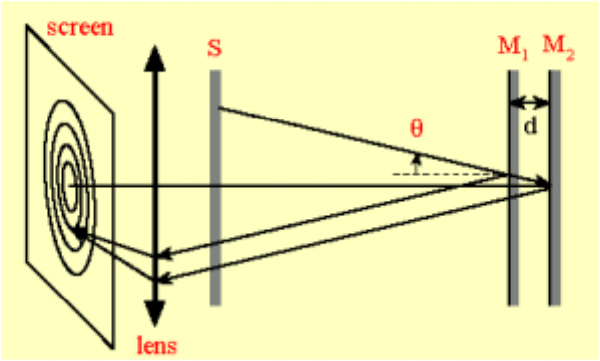

If the two mirrors are precisely aligned such that their planes are exactly perpendicular to one another, thus ensuring that path differences over different regions of the mirrors are constant, the fringe pattern will consist of a series of concentric rings. Each ring will correspond to a different angle of view, measured from the normal to the mirror M_1. These fringes are called fringes of equal inclination. They are analogous to fringes of equal inclination that we observe when we shine light from an extended source on a thin film. When the mirror M_1 is moved so as to approach the condition for zero path difference, the fringe pattern appears to collapse, with all fringes moving towards the center, and disappear.

Then reflection from the mirrors M_1 and M_2 is analogous to reflection from two surfaces of an air gap of thickness d. Since the phase shift upon reflection is the same for both mirrors, we find

$$2d\cos\theta = m\lambda$$

for constructive interference.

Differenza di cammino ottico che dà interferenza costruttiva

Formazione delle “frange” di interferenza può essere spiegata facendo riferimento a interferenza in riflessione multipla (cfr. Interferenza o diffrazione di Bragg, usata ad esempio in X-ray diffraction)

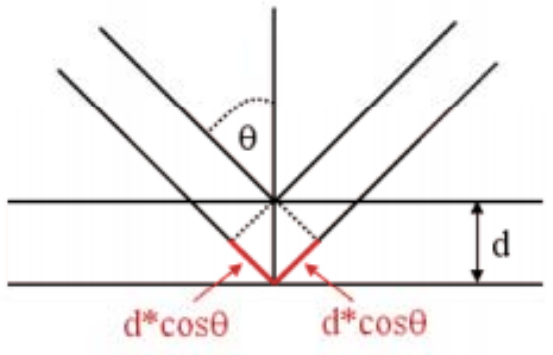

COERENZA I

Coerenza nasce da emissione stimolata (e, in genere, proveniente da piccolo volume di mezzo attivo)
Come si può caratterizzare meglio?

Definizioni di coerenza temporale e spaziale

The radiation emitted by an extended source S generates a total field amplitude A at the point P which is a superposition of an infinite number of partial waves with the amplitudes A_n and the phases ϕ_n emitted from the different surface elements dS (Fig.2.21), i.e.,

$$A(P) = \sum A_n(P)\, e^{i\phi n(P)} = \sum [A_n(0)/r_n^2]\, e^{i(\phi n_0 + 2\pi r_n/\lambda)}, \qquad (2.89)$$

where $\phi_{n0}(t) = \omega t + \phi_n(0)$ is the phase of the n^{th} partial wave at the surface element dS of the source. The phases $\phi_n(r_n,t)$ depend on the distances r_n from the source and on the angular frequency ω.

If the phase differences $\Delta\phi_n = \phi_n(P,t_1) - \phi_n(P,t_2)$ at a *given point* P between two different times t_1, t_2 are nearly the same for all partial waves, the radiation field at P is called *temporally coherent*. The maximum time intervall $\Delta t = t_2 - t_1$ for which $\Delta\phi_n$ for all partial waves differ by less than π is termed the *coherence time* of the radiation source. The path length $\Delta s_c = c\Delta t$ travelled by the wave during the coherence time Δt is the *coherence length*.

If a constant time-independent phase difference $\Delta\phi = \phi(P_1) - \phi(P_2)$ exists for the total amplitudes $A = A_0 e^{i\phi}$ at two different points P_1, P_2, the radiation field is called *spatially coherent*. All points P_m, P_n which fulfil the condition that for all times t, $|\phi(P_m,t) - \phi(P_n,t)| < \pi$, have nearly the same optical path difference from the source. They form the *coherence volume*.

The superposition of coherent waves results in interference phenomena which, however, can be observed directly only within the coherence volume. The dimensions of this coherence volume depend on the size of the radiation source, on the spectral width of the radiation and on the distance between source and observation point P.

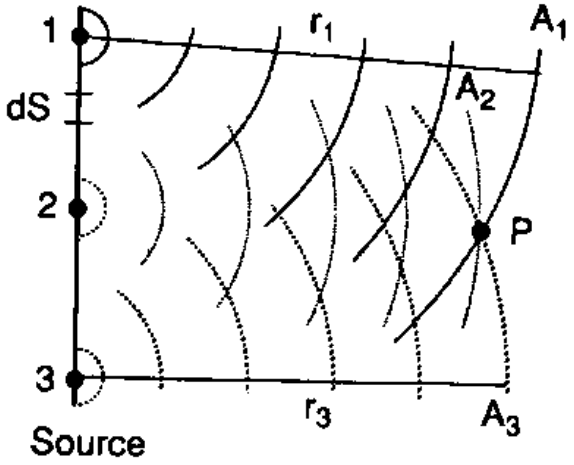

Fig.2.21. The field amplitudes A_n at a point P in a radiation field as superposition of an infinite number of waves from different surface elements dS_i of an extended source

Per l'interferenza è necessario avere luce coerente

PACCHETTI D'ONDA E MICHELSON

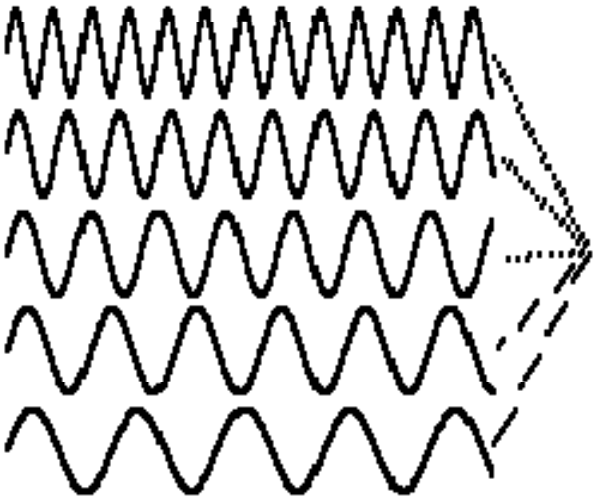

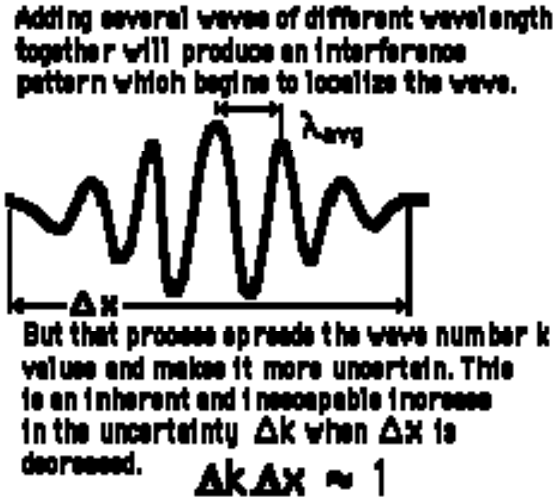

E, poiché la radiazione viaggia:

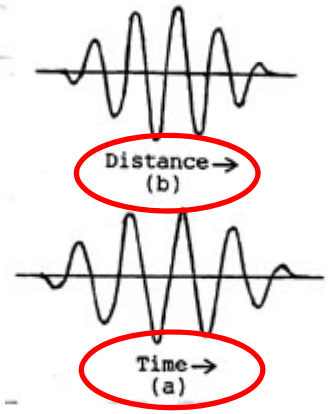

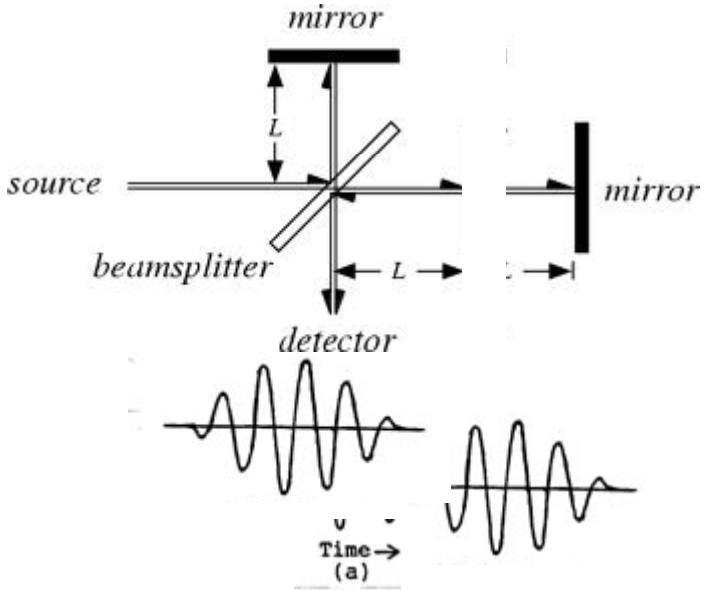

Se la differenza di cammino ottico è "troppo" grande, i pacchetti che hanno percorso I due cammini non si sovrapporranno
→ *la figura di interferenza scompare!!*

COERENZA II

2.7.1 Temporal Coherence

Consider a point source PS in the focal plane of a lens forming a parallel light beam which is divided by a beam splitter S into two partial beams (Fig. 2.22). They are superimposed in the plane of observation B after reflection from the mirrors M_1, M_2. This arrangement is called a *Michelson interferometer* (Sect.4.2). The two beams with wavelength λ travel different optical path lengths SM_1SB and SM_2SB, and their path difference in the plane B is

$$\Delta s = 2(SM_1 - SM_2) .$$

The mirror M_2 is mounted on a carriage and can be moved, resulting in a continuous change of Δs. In the plane B, one obtaines maximum intensity when both amplitudes have the same phase, which means $\Delta s = m\lambda$, and minimum intensity if $\Delta s = (2m+1)\lambda/2$. With increasing Δs, the contrast $(I_{max}-I_{min})/(I_{max}+I_{min})$ decreases and vanishes if Δs becomes larger than the coherence length Δs_c (Sect.2.7.4). Experiments show that Δs_c is related to the spectral width $\Delta\omega$ of the incident wave by

$$\Delta s_c \simeq c/\Delta\omega = c/(2\pi\Delta\nu) . \quad (2.90)$$

Lunghezza di coerenza

This observation may be explained as follows. A wave emitted from a point source with the spectral width $\Delta\omega$ can be regarded as a superposition of many quasi-monochromatic components with frequencies ω_n within the interval $\Delta\omega$. The superposition results in wave trains of finite length $\Delta s_c = c\Delta t = c/\Delta\omega$ because the different components with slightly different frequencies ω_n come out of phase during the time interval Δt and interfere destructively causing the total amplitude to decrease (Sect.3.1). If the path difference Δs in the Michelson interferometer becomes larger than Δs_c, the split wave trains no longer overlap in the plane B. The coherence lengths Δs_c of a light source therefore becomes larger with decreasing spectral width $\Delta\omega$.

Example 2.8

a) A low-pressure mercury spectral lamp with a spectral filter which only transmits the green line $\lambda = 546$ nm has, because of the Doppler width $\Delta\omega_D = 4\cdot10^9$ Hz, a coherence length of $\Delta s_c \simeq 8$ cm.

b) A single-mode HeNe laser with a bandwidth of $\Delta\nu = 1$ MHz has a coherence length of about 50 m.

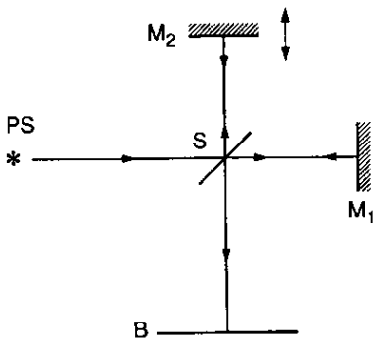

Fig.2.22. Michelson interferometer for measurements of the temporal coherence of radiation from the source S

Coerenza temporale del fascio essenziale per misure di interferometria Ad esempio: misure dimensionali (non invasive) di componenti meccanici con precisione nanometrica

Coerenza richiede monocromaticità!

COERENZA III

2.7.2 Spatial Coherence

The radiation from an *extended source* LS of size b illuminates two slits S_1 and S_2 in the plane A a distance d apart (Young's double-slit interference experiment, Fig.2.23a). The total amplitude and phase at each of the two slits are obtained by superposition of all partial waves emitted from the different surface elements df of the source, taking into account the different paths df-S_1 and df-S_2.

The intensity at the point of observation P in the plane B depends on the path difference S_1P-S_2P and on the phase difference $\Delta\phi = \phi(S_1)-\phi(S_2)$ of the total field amplitudes in S_1 and S_2. If the different surface elements df of the source emit independently with random phases (thermal radiation source) the phases of the total amplitudes in S_1 and S_2 will also fluctuate randomly. However, this would not influence the intensity in P as long as these fluctuations occur in S_1 and S_2 synchronously, because then the phase difference $\Delta\phi$ would remain constant. In this case, the two slits form two coherent sources which generate an interference pattern in the plane B.

For radiation emitted from the central part 0 of the light source this proves to be true since the paths $0S_1$ and $0S_2$ are equal and all phase fluctuations in 0 arrive simultaneously in S_1 and S_2. For all other points Q of the source, however, path differences $\Delta s_Q = QS_1 - QS_2$ exist, which are largest for the edges R of the source. From Fig.2.23b one can infer for $b << r$ the relation

$$\Delta s_R = R_1S_2 - R_1S_1 = R_2S_1 - R_1S_1 \simeq b\sin(\theta/2) .$$

For $\Delta s_R > \lambda/2$ the phase difference $\Delta\phi$ of the partial amplitudes in S_1 and S_2 exceeds π. With random emission from the different surface elements df of the source, the time-averaged interference pattern in the plane B will be washed out. The condition for coherent illumination of S_1 and S_2 from a light source with the dimension b is therefore

$$\Delta s = b\sin(\theta/2) < \lambda/2 .$$

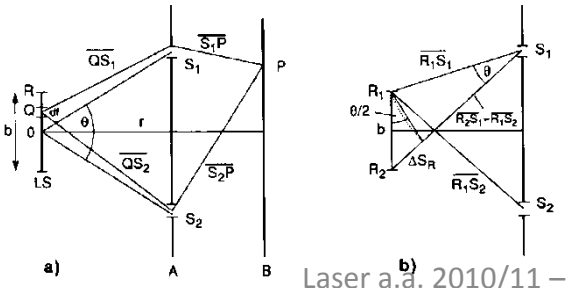

Fig.2.23a,b. Young's double-slit arrangement for measurements of spatial coherence

With $2\sin(\theta/2) = d/r$, this condition can be written as

$$bd/r < \lambda . \qquad (2.91a)$$

Extension of this coherence condition to two dimensions yields for a source area $A_s = b^2$ the following condition for the maximum surface $A_c = d^2$ which can be illuminated coherently:

$$b^2d^2/r^2 \leq \lambda^2 . \qquad (2.91b)$$

Since $d\Omega = d^2/r^2$ is the solid angle accepted by the illuminated surface $A_c = d^2$ this can be formulated as

$$A_s d\Omega \leq \lambda^2 . \qquad (2.91c)$$

The source surface $A_s = b^2$ determines the maximum solid angle $d\Omega \leq \lambda^2/A_s$ inside which the radiation field shows spatial coherence. Equation (2.91c) reveals that radiation from a point source (spherical waves) is spatially coherent within the whole solid angle $d\Omega = 4\pi$. The coherence surfaces are spheres with the source in the center. Likewise, a plane wave produced by a point source in the focus of a lens shows spatial coherence over the whole aperture confining the light beam. For given source dimensions, the coherence surface $A_c = d^2$ increases with the square of the distance from the source. Because of the vast distances to stars, the starlight received by telescopes is spatially coherent across the telescope aperture in spite of the large diameter of the radiation source.

The arguments above may be summarized as follows: The coherence surface S_c, i.e., that maximum area A_c which can be coherently illuminated at a distance r from an extended quasi-monochromatic light source with the area A_s emitting at a wavelength λ is determined by

$$S_c = \lambda^2 r^2/A_s . \qquad (2.92)$$

Superficie di coerenza

Superficie di coerenza: area che può essere illuminata con luce coerente

COERENZA IV

2.7.3 Coherence Volume

With the coherence length $\Delta s_c = c/\Delta\omega$ in the propagation direction of the radiation with the spectral width $\Delta\omega$ and the coherence surface $S_c = \lambda^2 r^2/A_s$ the coherence volume $V_c = S_c \Delta s_c$ becomes

$$V_c = \frac{\lambda^2 r^2 c}{\Delta\omega A_s} . \qquad (2.93)$$

Volume di coerenza

A unit surface element of a source with the spectral radiance L_ω [W/m^2·sterad] emits within the frequency interval $d\omega = 1$ Hz $L_\omega/\hbar\omega$ photons per second into the unit solid angle 1 sterad.

The mean number $\bar{n}$ of photons in the spectral range $\Delta\omega$ within the coherence volume defined by the solid angle $\Delta\Omega = \lambda^2/A_s$ and the coherence length $\Delta s_c = c\Delta t_c$ generated by a source with area A_s is therefore

$$\bar{n} = (L_\omega/\hbar\omega) A_s \Delta\Omega \Delta\omega \Delta t_c .$$

With $\Delta\Omega = \lambda^2/A_s$ and $\Delta t_c \simeq 1/\Delta\omega$ this gives

$$\bar{n} = (L_\omega/\hbar\omega)\lambda^2 . \qquad (2.94)$$

Example 2.9

For a thermal radiation source, the spectral radiance for linearly polarized light [(2.25) divided by a factor 2] is for $\cos\phi = 1$ and $L_\nu d\nu = L_\omega d\omega$

$$L_\nu = \frac{h\nu^3/c^2}{e^{h\nu/kT} - 1} .$$

The mean number of photons within the coherence volume is then with $\lambda = c/\nu$

$$\bar{n} = \frac{1}{e^{h\nu/kT} - 1} .$$

Esempio: sorgente termica (corpo nero)

This is identical to the mean number of photons per mode of the thermal radiation, as derived in Sect.2.2. Figure 2.5 and Example 2.3 give values of $\bar{n}$ for different conditions.

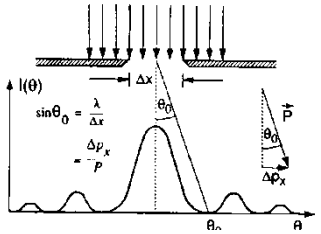

Fig.2.24. The uncertainty principle applied to the diffraction of light by a slit

The mean number $\bar{n}$ of photons per mode is often called the *degeneracy parameter* of the radiation field. This example shows that the coherence volume is related to the modes of the radiation field. This relation can be also illustrated in the following way:

If we allow the radiation from all modes with the same direction of $\mathbf{k}$ to escape through a hole in the cavity wall with the area $A_s = b^2$, the wave emitted from A_s will not be strictly parallel but will have a diffraction-limited divergence angle $\theta \simeq \lambda/b$ around the direction of $\mathbf{k}$. This means that the radiation is emitted into a solid angle $d\Omega = \lambda^2/b^2$. This is the same solid angle (2.91c) which limits the spatial coherence.

The modes with the same direction of $\mathbf{k}$ (which we assume to be the z direction) may still differ in $|\mathbf{k}|$, i.e., they may have different frequencies ω. The coherence length is determined by the spectral width $\Delta\omega$ of the radiation emitted from A_s. Since $|\mathbf{k}| = \omega/c$ the spectral width $\Delta\omega$ corresponds to an interval $\Delta k = \Delta\omega/c$ of the k values. This radiation illuminates a minimum "diffraction surface"

$$A_D = r^2 d\Omega = r^2\lambda^2/A_s .$$

Multiplication with the coherence length $\Delta s_c = c/\Delta\omega$ yields again the coherence volume $V_c = A_D c/\Delta\omega = r^2\lambda^2 c/(\Delta\omega A_s)$ of (2.93). We shall now demonstrate that the coherence volume is identical with the spatial part of the elementary cell in the general phase space.

As is well known from atomic physics, the diffraction of light can be explained by Heisenberg's uncertainty relation. Photons passing through a slit of width Δx have the uncertainty Δp_x of the x component p_x of their momentum $\mathbf{p}$, given by $\Delta p_x \Delta x \geq \hbar$ (Fig.2.24).

Generalized to three dimensions, the uncertainty principle postulates that the simultaneous measurements of momentum and location of a photon has the minimum uncertainty

$$\Delta p_x \Delta p_y \Delta p_z \Delta x \Delta y \Delta z \geq \hbar^3 = V_{ph} , \qquad (2.95)$$

where $V_{ph} = \hbar^3$ is the volume of one cell in phase space. *Photons within the same cell of the phase space are indistinguishable and can be therefore regarded as identical.*

Photons which are emitted from the hole $A_s = b^2$ within the diffraction angle $\theta = \lambda/b$ against the surface normal (Fig.2.25), which may point into the z direction, have the minimum uncertainty

$$\Delta p_x = \Delta p_y = |\mathbf{p}|\lambda/(2\pi b) = (\hbar\omega/c)\lambda/(2\pi b) = (\hbar\omega/c)d/(2\pi r) , \qquad (2.96)$$

of the momentum components p_x and p_y (the last equality follows from (2.91b).

COERENZA V

The uncertainty Δp_z is mainly caused by the spectral width $\Delta\omega$. Since $p = \hbar\omega/c$, we find

$$\Delta p_z = (\hbar/c)\Delta\omega \,. \qquad (2.97)$$

Substituting (2.96,97) into (2.95) we obtain for the spatial part of the phase-space cell

$$\Delta x \Delta y \Delta z = \frac{\lambda^2 r^2 c}{\Delta\omega A_s} = V_c \,,$$

which turns out to be identical with the coherence volume defined by (2.93).

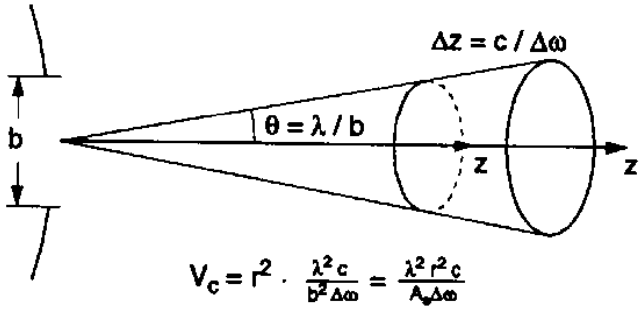

Fig.2.25. Coherence volume and phase space cell

44

Volume di coerenza rappresenta regione (spaziale) in cui i fotoni si comportano allo stesso modo

Rozzamente, volume di coerenza dipende da:
- Area di coerenza ← spazio delle fasi reale
- Lunghezza di coerenza ← tempo coerenza ← monocromaticità

Fotoni emessi da piccolo volume di mezzo attivo per emissione stimolata appartengono alle stesse celle dello spazio delle fasci, cioè sono indistinguibili (quantisticamente)

Nota: luce coerente può essere efficacemente focalizzata
(è un time reversal rispetto alla generazione), con il solo limite della diffrazione

POTENZA ED INTENSITÀ LASER

Molte applicazioni dei laser dipendono da elevate intensità
Oltre a coerenza (direzionalità e possibilità di focalizzare), intensità dipende da carattere amplificatore di mezzo attivo

Potenze *tipiche* di alcuni laser CW (in continua):
-HeNe: 1-50 mW
-Ar^+: 0.1-10 W
-CO_2: 10 W- kW
-Nd:YAG (e simili): 5-50 W
-Diodo: 10 mW – 10 W ("barrette")

Limitazioni tecnologiche per la potenza:
- Efficienza pompaggio (valori tipici 1-10%);
- Complicati sistemi accessori (raffreddamento, alimentazione, controllo, etc.);
- Densità del mezzo attivo (al massimo idealmente vengono emessi n/τ fotoni/(volume secondo)
- Volume del mezzo attivo (conviene sia piccolo per aumentare coerenza spaziale)
- Robustezza del mezzo attivo (il mezzo attivo è interessato da potenze paragonabili a quelle di emissione)

Limitazione fisica per la potenza:
$-\Delta N \rightarrow \Delta N_{thr}$ in condizioni stazionarie
→ guadagno tende a un limite

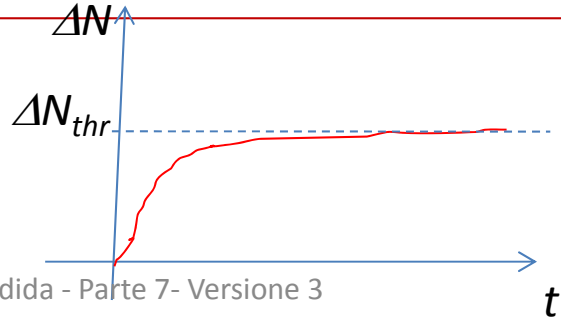

BRILLANZA

1.4.4. Brightness

We define the brightness of a given source of em waves as the power emitted per unit surface area per unit solid angle. To be more precise let dS be the elemental surface area at point O of the source (Fig. 1.7a). The power dP emitted by dS into a solid angle $d\Omega$ around direction OO' can be written as:

$$dP = B \cos\theta \, dS \, d\Omega \tag{1.4.3}$$

where θ is the angle between OO' and the normal $\mathbf{n}$ to the surface. Note that the factor $\cos\theta$ occurs because the physically important quantity for emission along the OO' direction is the projection of dS on a plane orthogonal to the OO' direction, i.e., $\cos\theta \, dS$. The quantity B defined through Eq. (1.4.3) is called the *source brightness* at point O in the direction OO'. This quantity generally depends on polar coordinates θ and ϕ of the direction OO' and on point O. When B is a constant, the source is said to be isotropic (or a Lambertian source).

Let us now consider a laser beam of power P, with a circular cross section of diameter D and with a divergence θ (Fig. 1.7b). Since θ is usually very small, we have $\cos\theta \cong 1$. Since the area of the beam is equal to $\pi D^2/4$ and the emission solid angle is $\pi\theta^2$, then, according to Eq. (1.4.3), we obtain the beam brightness as:

$$B = \frac{4P}{(\pi D\theta)^2} \tag{1.4.4}$$

Note that, if the beam is diffraction limited, we have $\theta = \theta_d$, and, with the help of Eq. (1.4.1), we obtain from Eq. (1.4.4):

$$B = \left(\frac{2}{\beta\pi\lambda}\right)^2 P \tag{1.4.5}$$

β : fattore geometrico ~ 1

which is the maximum brightness for a beam of power P.

Brightness is the most important parameter of a laser beam and, in general, of any light source. To illustrate this point we first recall that, if we form an image of any light source through a given optical system and if we assume that the object and image are in the same medium (e.g., air), then the following property holds: The brightness of the image is always less than or equal to that of the source, the equality holding when the optical system provides lossless imaging of the light emitted by the source. To illustrate further the importance of

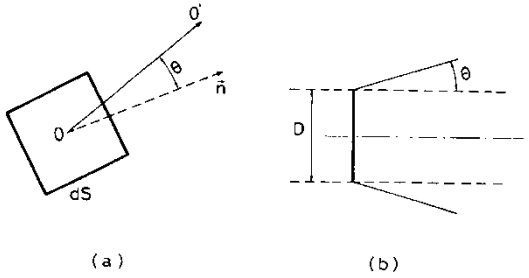

FIG. 1.7. (a) Surface brightness at the point O for a general source of em waves. (b) Brightness of a laser beam of diameter D and divergence θ.

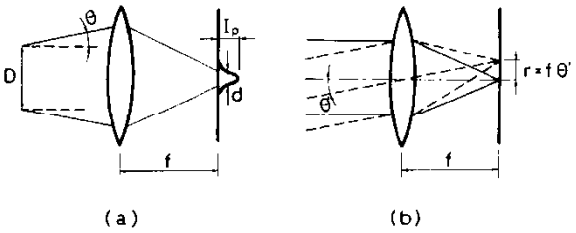

FIG. 1.8. (a) Intensity distribution in the focal plane of a lens for a beam of divergence θ. (b) Plane wave decomposition of the beam in (a).

brightness, let us consider the beam in Fig. 1.7b, with divergence equal to θ, to be focused by a lens of focal length f. We are interested in calculating the peak intensity of the beam in the focal plane of the lens (Fig. 1.8a). To make this calculation we recall that the beam can be decomposed into a continuous set of plane waves with an angular spread of approximately θ around the propagation direction. Two such waves, making an angle θ', are indicated by solid and dashed lines, respectively, in Fig. 1.8b. The two beams are each focused on a distinct spot in the focal plane, and, for a small angle θ', the two spots are transversly separated by a distance $r = f\theta'$. Since the angular spread of the plane waves that make up the beam in Fig. 1.8a equals the beam divergence θ, we conclude that the diameter d of the focal spot in Fig. 1.8a is approximately equal to $d = 2f\theta$. For an ideal lossless lens, the overall power in the focal plane equals the power P of the incoming wave. The peak intensity in the focal plane is thus $I_p = 4P/\pi d^2 = P/\pi(f\theta)^2$. In terms of beam brightness, according to Eq. (1.4.4), we then have $I_p = (\pi/4)B(D/f)^2$. Thus I_p increases with increasing beam diameter D. The maximum value of I_p is then attained when D is made equal to the lens diameter D_L. In this case we obtain

$$I_p = \left(\frac{\pi}{4}\right)(N.A.)^2 B \tag{1.4.6}$$

where $N.A. = \sin[\tan^{-1}(D_L/f)] \cong (D_L/f)$ is the lens numerical aperture. Equation (1.4.6) then shows that, for a given numerical aperture, the peak intensity in the focal plane of a lens depends only on beam brightness.

A laser beam of even moderate power (e.g., a few milliwatts) has a brightness several orders of magnitude greater than that of the brightest conventional sources (see, e.g., Problem 1.7). This is mainly due to the highly directional properties of the laser beam. According to Eq. (1.4.6) this means that the peak intensity produced in the focal plane of a lens can be several orders of magnitude greater for a laser beam compared to that of a conventional source. Thus the intensity of a focused laser beam can reach very large values, a feature exploited in many applications of lasers.

Es.: HeNe, 1mW, 633nm: B~10^9 W/m^2
I_P>10^4 W/cm^2~$3x10^{22}$ fotoni/(s cm^2)
[>> densità superficiale tipica materia]

INTERFEROMETRIA E METROLOGIA I

Displacement interferometry

http://www.laserfocusworld.com/articles/print/volume-41/issue-12/features/nanometrology-controlling-error-sources-yields-nano-accurate-interferometry.html

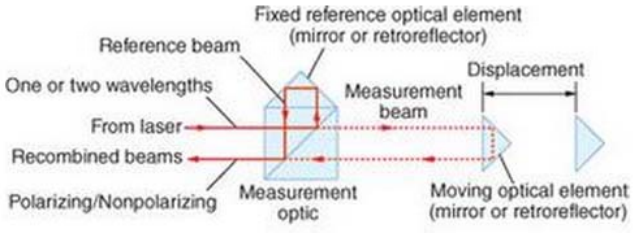

FIGURE 2. Displacement interferometry is performed in a classical Michelson interferometer setup in which the plane mirrors are replaced by retroreflectors, also called corner cubes. The optics can be polarizing or nonpolarizing, although polarizing optics are most common.

Displacement interferometry

Displacement interferometry is based on the light-dark transitions corresponding to constructive and destructive interference (see Fig. 2). Homodyne interferometers work with only one frequency, while heterodyne interferometers work with two frequencies. Both types ultimately measure a displacement *d*, which is counted as a number *N* of half wavelengths λ plus a fraction that is usually called the phase change Δφ. The displacement *d* is given by:

$$d = \frac{\lambda}{2} \cdot \left(N + \frac{\Delta\varphi}{2\pi} \right)$$

Click here to enlarge image

Sensibilità nanometrica!!

Cause di errore…

The equation indicates the major error sources: the wavelength, the count number, and the phase difference. In modern systems, the resolution generally falls between 10 and 0.1 nm.

Two potential sources of error in displacement interferometry are related to alignment. The first-order alignment error, Abbe error, appears when the measurement axis and the axis along which the displacement must be known are not in line. For small rotational errors of the moving member, the error is equal to the rotational error times the distance between the axes, also called the "Abbe arm."

The second-order alignment error is called cosine error, because its magnitude is proportional to the cosine of the angle between the intended alignment and the actual alignment. For the typical small angles this works as a second-order effect as the cosine approaches unity with the square of the angle. On one hand this means that good alignment can keep the effect negligible, on the other hand the effect is hard to correct once it occurs. An alignment error of 1 mm/m, for example, gives a relative deviation of 5×10^{-7} in the measured displacement.

INTERFEROMETRIA E METROLOGIA II

Additional displacement error sources

Wavelength can present another source of error in displacement interferometry. The wavelength λ depends on the frequency *f* and the refractive index of air *n* and is given by

$$\lambda = \frac{c}{n \cdot f}$$

Click here to enlarge image

where c is the speed of light. The refractive index of air depends on the air pressure, temperature, humidity, and CO_2 content. Once these data are known, there are standard equations for calculating the refractive index with an uncertainty on the order of 10^{-8}.[1] The deviation in each of the environmental parameters that correspond to a measurement deviation of 1×10^{-6} in length are 4 hPa for pressure, 1.1°C for air temperature, 100% for humidity, and 0.6% CO_2 for content.

The latter two values are unrealistic, however, because these factors only become important for uncertainties far below 1×10^{-6}. The frequency *f* is usually obtained from a stabilized He-Ne laser source with a stability of less than 1×10^{-8}. And because the commonly used stabilization techniques are well developed, they seldom present problems. If the source is a laser diode this can be a point of concern, however.

Metrologia di spostamento permette misure molto accurate, ma richiede di rimuovere cause di errore fra cui:

- Allineamenti;
- Stabilità condizioni operative (e.g., fluttuazioni indice di rifrazione);
- Stabilità frequenza (cfr. Jitter nell'operazione multimodo di un laser)

RICHIAMI DI EFFETTO DOPPLER

Nella interferometria di spostamento c'è un oggetto in movimento!!

The **Doppler effect** (or **Doppler shift**), named after Austrian physicist Christian Doppler who proposed it in 1842 in Prague, is the change in frequency of a wave for an observer moving relative to the source of the wave. It is commonly heard when a vehicle sounding a siren or horn approaches, passes, and recedes from an observer. The received frequency is higher (compared to the emitted frequency) during the approach, it is identical at the instant of passing by, and it is lower during the recession.

The relative changes in frequency can be explained as follows. When the source of the waves is moving toward the observer, each successive wave crest is emitted from a position closer to the observer than the previous wave. Therefore each wave takes slightly less time to reach the observer than the previous wave. Therefore the time between the arrival of successive wave crests at the observer is reduced, causing an increase in the frequency. While they are travelling, the distance between successive wave fronts is reduced; so the waves "bunch together". Conversely, if the source of waves is moving away from the observer, each wave is emitted from a position farther from the observer than the previous wave, so the arrival time between successive waves is increased, reducing the frequency. The distance between successive wave fronts is increased, so the waves "spread out".

Nota: questa figura e ciò che essa sottende valgono solo per onde longitudinali (e.g., acustiche), ma il concetto vale anche per onde e.m.

La radiazione riflessa dall'oggetto viene shiftata in frequenza in modo proporzionale alla velocità:
$|f/f_0| = v/c$

In classical physics, where the speeds of source and the receiver relative to the medium are lower than the velocity of waves in the medium, the relationship between observed frequency f and emitted frequency f_0 is given by:[3]

$$f = \left(\frac{c + v_r}{c - v_s}\right) f_0$$

where

c is the velocity of waves in the medium

v_r is the velocity of the receiver relative to the medium; positive if the receiver is moving towards the source.

v_s is the velocity of the source relative to the medium; positive if the source is moving away from the receiver.

The frequency is decreased if either is moving away from the other.

RICHIAMI DI BATTIMENTO

If two laser beams with different optical frequencies are superimposed on a photodetector measuring the optical intensity, a beat note – i.e., a signal with the difference of the optical frequencies – can usually be observed, if some conditions are met:

- The spatial distributions of the two light fields must not be orthogonal. Somewhat clipping the beams, or even just some non-uniformity of the detector surface, can solve this problem.
- The polarization states also must not be orthogonal.
- The optical frequency difference must be within the bandwidth of the detector.
- Obviously, the wavelengths must be within the range where the photodetector is sensitive.

$$f_{beat} = f_1 - f_2$$

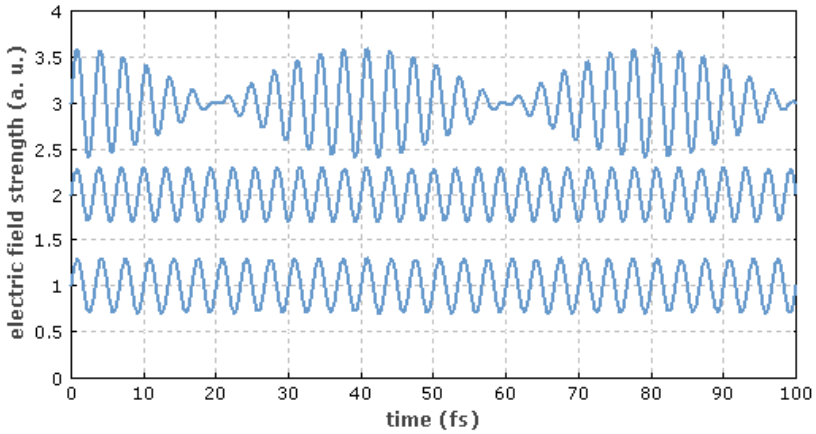

Figure 1: Superposition of two optical oscillations with a frequency difference of 25 THz. The bottom two curves show the electric field strengths of the isolated oscillations, and the to curve the additive superposition. A sufficiently fast intensity detector would record an oscillation of the power with the difference frequency.

$$\sin(2\pi f_1 t) + \sin(2\pi f_2 t) = 2\cos\left(2\pi\frac{f_1 - f_2}{2}t\right)\sin\left(2\pi\frac{f_1 + f_2}{2}t\right)$$

A physical interpretation is that when $\cos\left(2\pi\frac{f_1 - f_2}{2}t\right)$ equals one, the two waves are in phase and they interfere

La sovrapposizione di onde di frequenza diversa (e relazione di fase assegnata) dà luogo a **battimenti**, cioè alla modulazione temporale, a frequenza differenza, dell'ampiezza

INTERFEROMETRI OMODINA

Homodyne laser systems

A single frequency laser source is used in homodyne systems (see Figure 3), which results in an outbound beam with a single frequency F_1. The laser beam from the stationary reference path is returned with frequency F_1 but the beam from the moving measurement path is returned with a Doppler shifted frequency of $F_1 \pm \delta F$.

These beams are interfered together in the detector to give a beat frequency of zero when the optics are stationary, whilst the beat frequency rises as the optics move in either direction. The direction of motion is detected from the signal phase change. Unlike heterodyne systems, high resolution position sensing requires stable measurement of signal voltage.

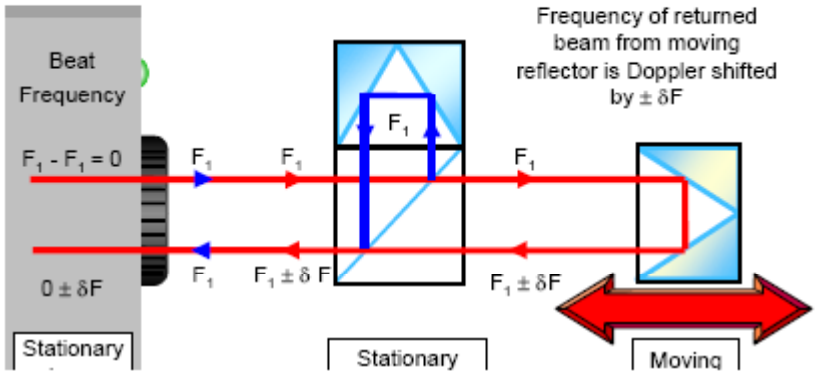

Figure 3 - homodyne laser system operation

Figure

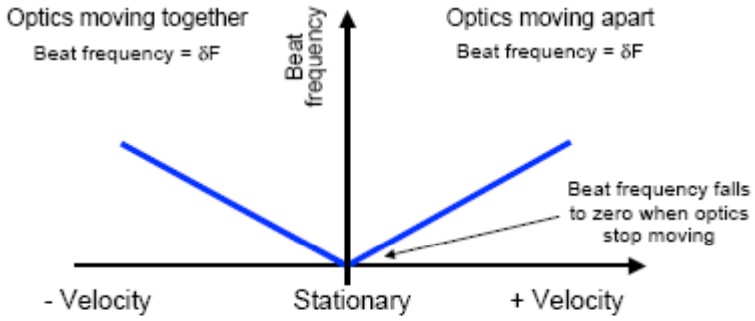

Figure 4 – homodyne system: beat frequency vs. velocity

INTERFEROMETRI ETERODINA

Heterodyne laser systems

Figure 1 shows a heterodyne laser system. The output beam from the dual frequency laser source contains two polarisations, one with a frequency F_1 , the other with frequency F_2. The beat frequency between them is $F_2 - F_1$. A polarising beam-splitter reflects the light with frequency F_1 into the reference path. Light with frequency F_2 passes through the splitter into the measurement path where it strikes the moving reflector causing the frequency of the reflected beam to be Doppler shifted by $\pm\delta F$. This reflected beam is then combined with the F_1 frequency light at the interferometer, and returned to the laser detector unit with a new beat frequency of $F_2 - F_1 \pm \delta F$.

Figure 2 shows how the beat frequency of a heterodyne laser system varies with the velocity of the moving reflector. When the optics are stationary, the beat frequency is $F_2 - F_1$. As the optics move apart, the beat frequency rises by δF, if they move together it falls. High-resolution position sensing therefore requires stable measurement of signal phase, whilst a velocity limit occurs as the beat frequency approaches d.c.

therefore requires stable measurement of signal phase, whilst a velocity limit occurs as the beat frequency approaches d.c.

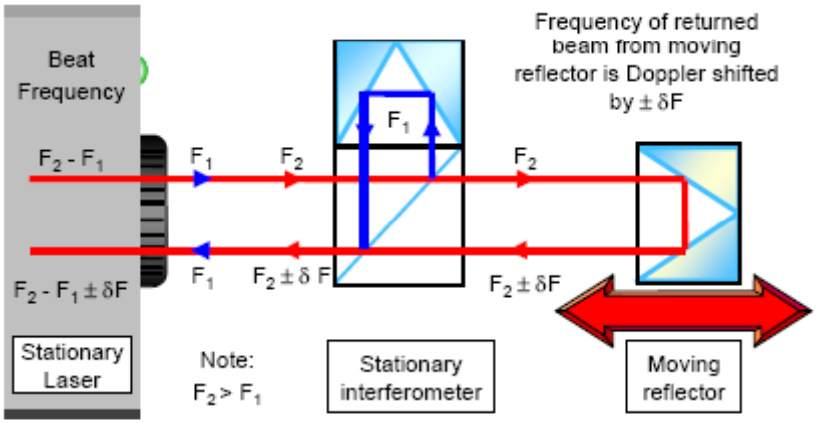

Figure 1 - heterodyne laser system operation

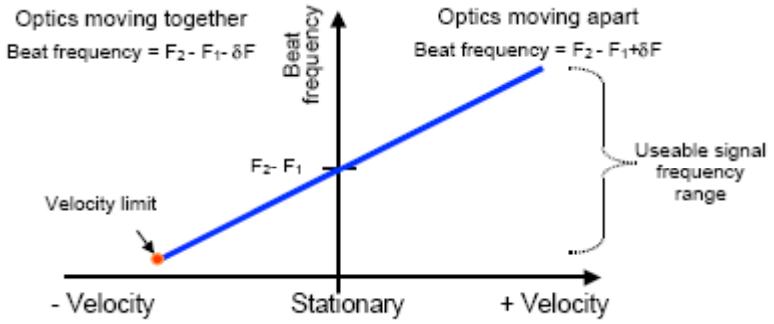

Figure 2 - heterodyne system: beat frequency vs. velocity

Può essere più conveniente misurare la variazione di frequenza di un battimento prestabilito che la frequenza del battimento stesso (permette di misurare lo sfasamento, cosa più sensibile e meno rumorosa della misurazione di ampiezze)

MODULATORI ACUSTO-OTTICI (AOM)

An **acousto-optic modulator (AOM)**, also called a **Bragg cell**, uses the acousto-optic effect to diffract and shift the frequency of light using sound waves (usually at radio-frequency). They are used in lasers for Q-switching, telecommunications for signal modulation, and in spectroscopy for frequency control. A piezoelectric transducer is attached to a material such as glass. An oscillating electric signal drives the transducer to vibrate, which creates sound waves in the glass. These can be thought of as moving periodic planes of expansion and compression that change the index of refraction. Incoming light scatters (see Brillouin scattering) off the resulting periodic index modulation and interference occurs similar to in Bragg diffraction. The interaction can be thought of as four-wave mixing between phonons and photons. The properties of the light exiting the AOM can be controlled in five ways:

1. Deflection

A diffracted beam emerges at an angle θ that depends on the wavelength of the light λ relative to the wavelength of the sound Λ

$$\sin\theta = \left(\frac{m\lambda}{2\Lambda}\right)$$

in the Bragg regime and

$$\sin\theta = \left(\frac{m\lambda_0}{n\Lambda}\right)$$

with the light : normal to the sound waves, where
m = ..., −2, −1, 0, 1, 2, ... is the order of diffraction.

M080-2G-LV1

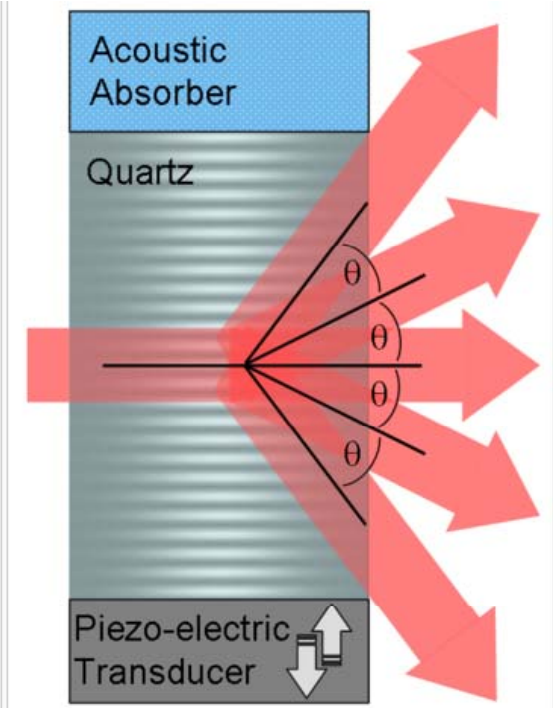

An acousto-optic modulator consists of a piezoelectric transducer which creates sound waves in a material like glass or quartz. A light beam is diffracted into several orders. By vibrating the material with a pure sinusoid and tilting the AOM so the light is reflected from the flat sound waves into the first diffraction order, up to 90% deflection efficiency can be achieved.

3. Frequency

One difference from Bragg diffraction is that the light is scattering from moving planes. A consequence of this is the frequency of the diffracted beam f in order m will be Doppler-shifted by an amount equal to the frequency of the sound wave F.

$$f \rightarrow f + mF$$

This frequency shift is also required by the fact that energy and momentum (of the photons and phonons) are conserved in the process. A typical frequency shift varies from 27 MHz, for a less-expensive AOM, to 400 MHz, for a state-of-the-art commercial device. In some AOMs, two acoustic waves travel in opposite directions in the material, creating a standing wave. Diffraction from the standing wave does not shift the frequency of the diffracted light.

INTERFEROMETRIA DI SUPERFICIE

Surface interferometry

Surface interferometry-which can be carried out in classical Michelson and Fizeau setups-can be considered as a kind of displacement interferometry. Key differences are that an array of photodetectors (like a CCD camera) is used, and the (static) phase difference among several areas on the surface is taken to represent the surface features (see Fig. 3). In this case, the equation on p. 87 is valid for the distance between the reference surface and the surface to be measured as shown in Fig. 2. For an optimum contrast, the intensity is proportional to:

$$I \propto 1 + \cos\frac{2\pi}{\lambda}(\Delta z);$$

$$I(x,y) \propto 1 + \cos[\varphi(x,y)];$$

$$\text{with } \varphi(x,y) = \frac{2\pi z(x,y)}{\lambda}$$

Click here to enlarge image

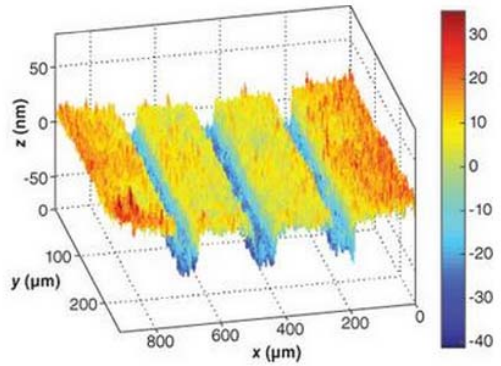

Several methods can be used to determine the surface structure $z(x,y)$. One method is essentially similar to homodyne interferometry, except that CCD cameras are used instead of photodetectors. This method is called instantaneous phase shifting because it takes a very short measuring time and there is no time difference between images taken with a different phase shift.[4]

More commonly used is temporal phase shifting. The reference mirror is displaced over a half wavelength in five (or more) steps, and the phase per pixel is derived from the various intensities.[5] In these cases the interference number N remains undetermined and unimportant. When the phase passes 360°, however, it should continue instead of starting at zero again. The process of removing these discontinuities, a separate subject, is referred to as phase unwrapping.

A third way to determine the surface heights is to consider the whole interference pattern. The reference plane is tilted to guarantee a constant number of fringes, which results in fringes with a determined spatial frequency or carrier frequency. Surface deviations give deviations in this spatial frequency that can be converted to height differences by a Fourier transform and additional manipulations. This method is referred to as the carrier-fringe method, and compared to the other methods it has relatively limited lateral resolution. [6]

Qui non ci sono oggetti in movimento ma si esegue un raffronto (interferenza!) tra un cammino ottico di riferimento e quello che prevede la riflessione dalla superficie

INTERFEROMETRO DI FIZEAU

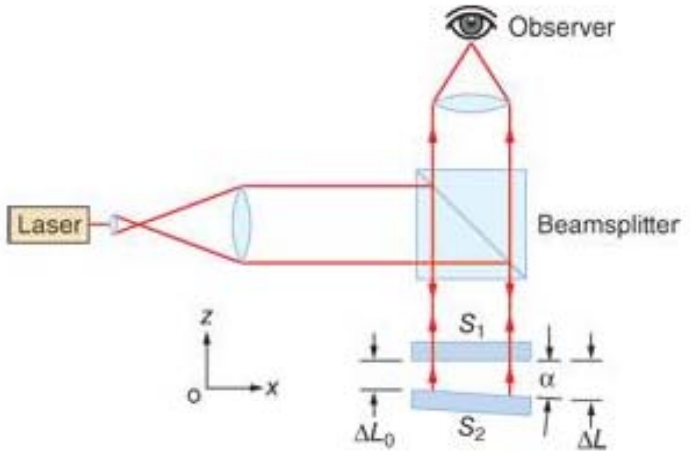

FIGURE 3. In a Fizeau interferometer, the light reflected from the upper side of test mirror S2 interferes with the light reflected from the lower side of reference mirror S1.

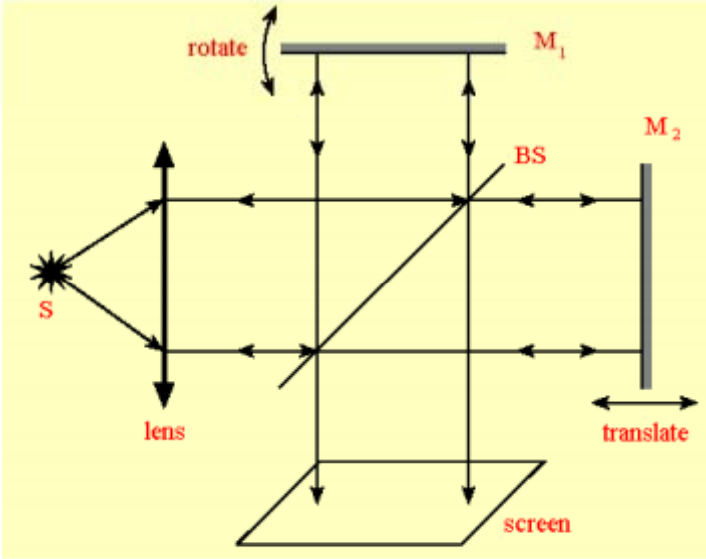

Error sources in surface interferometry

The basic error source in surface interferometry is the reference surface. All measurements refer to this surface. Methods exist to make or to approximate an absolute flatness calibration, but are limited by various error sources.[7]

Because the range of distances is small, wavelength and atmospheric conditions exert little effect on the measurement result in terms of the height between highest and lowest point on the surface. And a relative uncertainty of 10^{-6} is well within a nanometer. In this case the dead path error, as described for displacement interferometry, becomes dominant. Perturbations in the air between the reference surface and the surface to be measured cause these deviations over the whole length of the gap. In the phase-stepping method, this can be reflected in poor contrast and problems with phase unwrapping. In the other two methods this perturbation is frozen in the calculated surface, where the user does not notice it.

Periodic errors can appear in surface interferometry from sources that include nonlinearity in detectors, incorrect and unequal steps in the phase-shifting methods, and atmospheric perturbations during the phase steps. In the carrier-fringe methods, all problems with the Fourier transform, such as signal leaking and aliasing will give mainly periodic errors.

Errors in microscopic interferometry

Microscopic interferometry has error sources essentially similar to those for displacement and surface interferometry. In monochromatic interferometry, the effective wavelength must be carefully observed, as beams are strongly convergent. The correction for this effect is called aperture correction and depends on the numerical aperture of the microscope objective. In white-light interferometry, the light no longer has a defined wavelength, but is used for zero detection. The height information comes from an independent length scale in the system, and therefore introduces the errors contained in that system (Abbe errors, for instance).❑

Twyman-Green Interferometer

The Twyman-Green interferometer is a very useful instrument for measuring defects in optical components such as lenses, prisms, plane-parallel windows, laser rods, and plane mirrors. The beam splitter and mirror arrangement of the Twyman-Green interferometer resembles that of a Michelson interferometer. The difference lies in the way the interferometers are illuminated. While the Michelson interferometer is used with an extended light source, the Twyman-Green interferometer is used with a monochromatic point source which is located at the principal focus of a well-corrected lens.

INTERFEROMETRIA A LUCE BIANCA I

White Light Interferometry

James C. Wyant
Optical Sciences Center, University of Arizona, Tucson, AZ 85721
jcwyant@optics.arizona.edu, http://www.optics.arizona.edu/jcwyant

Currently most interferometry is performed using a laser as the light source. The primary reason for this is that the long coherence length of laser light makes it easy to obtain interference fringes and interferometer path lengths no longer have to be matched as they do if a short coherence length white light source is used. The ease with which interference fringes are obtained when a white light source is used is both good and bad. It is good that it is easy to find laser light interference fringes, but it can be bad in that it can be too easy to obtain interference fringes and any stray reflections will give spurious interference fringes. Spurious interference fringes can result in incorrect measurements.

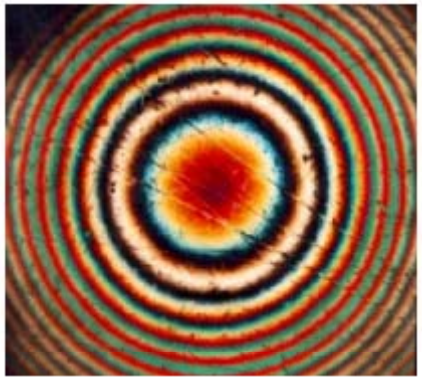

Figure 1. White light interference fringes.

3. VERTICAL SCANNING OR COHERENCE PROBE INTERFEROMETERS

Phase-shifting interferometry has proven to be extremely powerful and useful and many commercial interferometers use phase-shifting techniques. While phase-shifting interferometry has great precision, it has limited dynamic range. It can easily be shown that for phase-shifting interferometry the height difference between two adjacent data points must be less than $\lambda/4$, where λ is the wavelength of the light used. If the slope is greater than $\lambda/4$ per detector pixel then height ambiguities of multiples of half-wavelengths exist as shown in Figure 3. One technique that has been very successful in overcoming these slope limitations is to perform the measurement using two or more wavelengths. If measurements are performed using two wavelengths, λ_1 and λ_2, it can be shown that the maximum height difference between two consecutive data points is $\lambda_{eq}/4$, where λ_{eq} is given by

$$\lambda_{eq} = \frac{\lambda_1 \lambda_2}{|\lambda_1 - \lambda_2|}$$

Thus, by carefully selecting the two wavelengths it is possible to greatly increase the dynamic range of the measurement over what can be obtained using a single wavelength. (9-11).

Usando una singola frequenza, si ricostruisce la modulazione topografica "modulo $\lambda/4$"

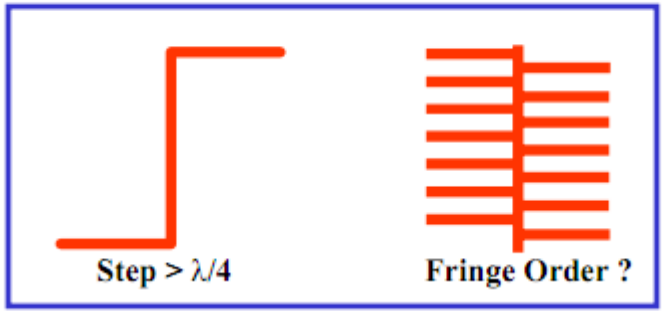

Figure 3. If a single wavelength is used and the phase step is greater than $\lambda/4$ it is difficult to connect the fringe orders on the two sides of the step.

INTERFEROMETRIA A LUCE BIANCA II

A better approach is to use a white light source so there is no ambiguity in the fringe order number as shown in Figure 4.

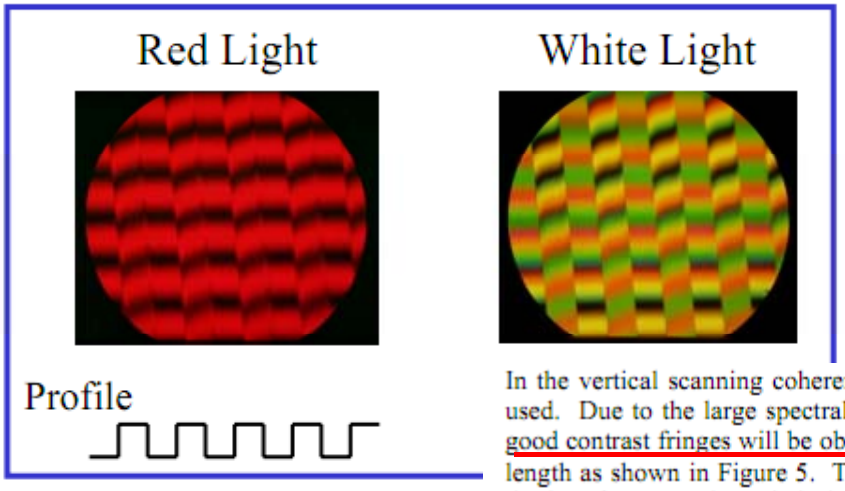

Figure 4. The use of white light makes it possible to connec
height is greater than λ/4.

In the vertical scanning coherence peak sensing mode of operation a broad spectral width light source is used. Due to the large spectral bandwidth of the source, the coherence length of the source is short, and good contrast fringes will be obtained only when the two paths of the interferometer are closely matched in length as shown in Figure 5. Thus, if in the interference microscope the path length of the sample arm of the interferometer is varied, the height variations across the sample can be determined by looking at the sample position for which the fringe contrast is a maximum. In this measurement there are no height ambiguities and since in a properly adjusted interferometer the sample is in focus when the maximum fringe contrast is obtained, there are no focus errors in the measurement of surface microstructure (12-16).

A causa della piccola lunghezza di coerenza, si vedono le frange solo se le distanze sono "matchate" → *necessario variare la posizione del campione in modo controllato (traslatori PZT)*

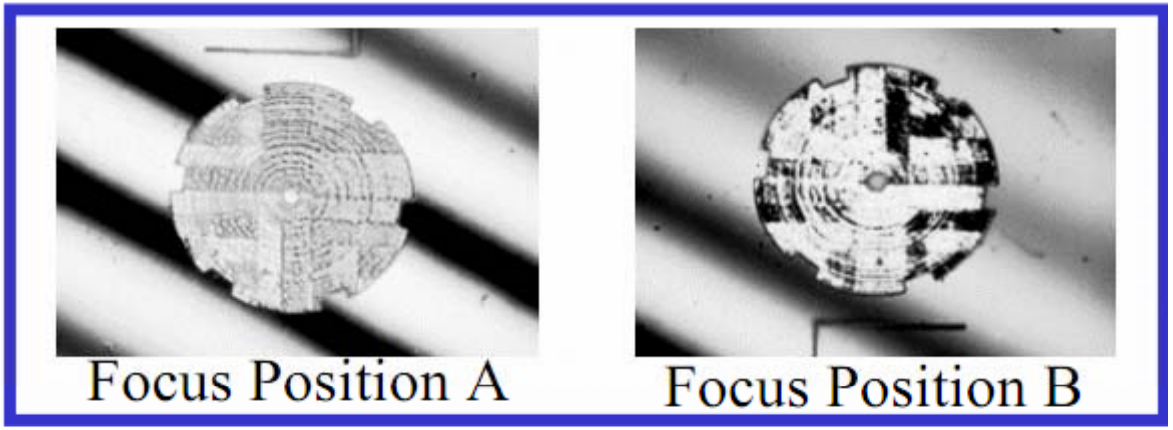

Figure 5. Good contrast fringes are obtained only when the interferometer paths are matched. (Sample is a micro-machined piece of silicon.)

INTERFEROMETRIA A LUCE BIANCA III

The major drawback of this type of scanning interferometer measurement is that only a single surface height is being measured at a time and a large number of measurements and calculations are required to determine a large range of surface height values. One method for processing the data that gives both fast and accurate measurement results is to use conventional communication theory and fast computers with efficient software to demodulate the envelope of the fringe signal to determine the peak of the fringe contrast.

Figure 6 shows the irradiance at a single sample point as the sample is translated through focus. It should be noted that this signal looks a lot like an amplitude modulated (AM) communication signal. To obtain the location of the peak, and hence the surface height information, this irradiance signal is detected using a CCD array. The signal is sampled at fixed intervals, such as every 80 or 240 nm, as the sample path is varied. Low frequency and DC signal components are removed from the signal by digital high pass filtering. The signal is next rectified by square-law detection and digitally low pass filtered. The peak of the low pass filter output is located and the vertical position corresponding to the peak is noted. Interpolation between sample points can be used to increase the resolution of the instrument beyond the sampling interval. This type of measurement system produces fast, non-contact, true three-dimensional area measurements for both large steps and rough surfaces to nanometer precision.

Necessario sviluppare tecniche di manipolazione dati sofisticate

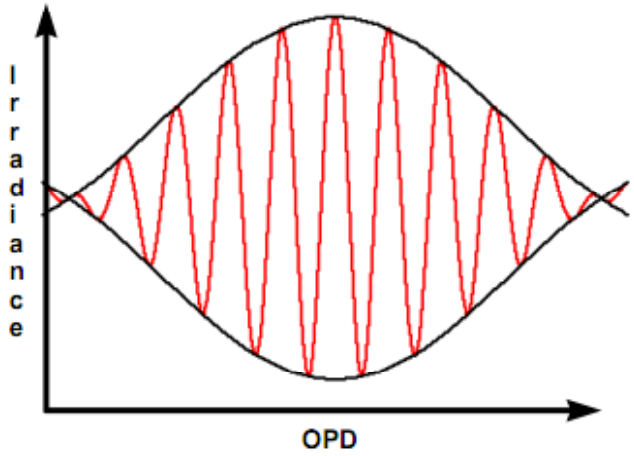

Figure 6. Irradiance at a single sample point as the sample is translated through focus.

Cambiando la posizione verticale dell'oggetto si osserva una sorta di battimento!

COHERENCE PEAK SENSING MICROSCOPE I

Figure 7 shows a simplified schematic of a coherence peak sensing interference microscope. The configuration shown in Figure 7 utilizes a two-beam Mirau interferometer at the microscope objective. Typically the Mirau interferometer is used for magnifications between 10 and 50X, a Michelson interferometer is used for low magnifications, and the Linnik interferometer is used for high magnifications. A separate magnification selector is placed between the microscope objective and the CCD camera to provide additional image magnifications. A tungsten halogen lamp is used as the light source. Light reflected from the test surface interferes with light reflected from the reference. The resulting interference pattern is imaged onto the CCD array. Also, output from the CCD array is digitized and read by the computer. The Mirau interferometer is mounted on either a piezoelectric transducer (PZT) or a motorized stage so that it can be moved. During this movement, the distance from the lens to the reference surface remains fixed. Thus, a phase shift is introduced into one arm of the interferometer. By introducing a phase shift into only one arm while recording the interference pattern that is produced, it is possible to perform either phase-shifting interferometry or vertical scanning coherence peak sensing interferometry.

Figure 8 shows typical results obtained measuring a micro-machined piece of silicon.

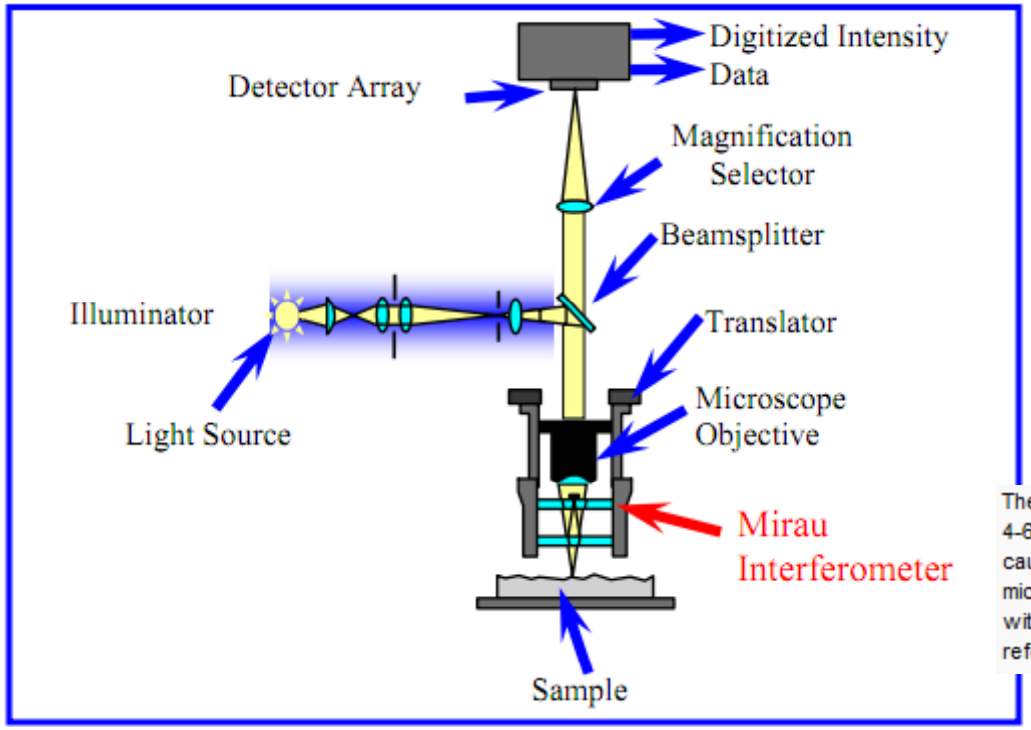

Figure 7. Optical schematic of interference microscope used for measurement of fine surface structure.

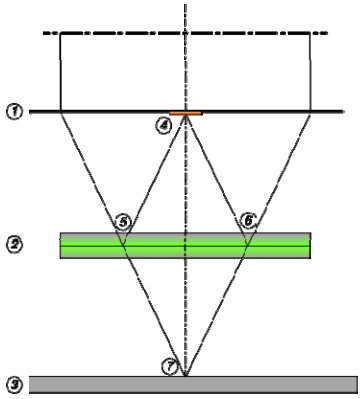

The figure shows the optical path of a Mirau-interferometer. Reference beam (5-4-6) and object beam (5-7-6) have identical optical path length and can thus cause white light interference. Parts of the Mirau interferometer: 1. Lens of the microscope, 2. Semitransparent mirror, 3. Object surface, 4. Reference mirror with reference beam, 5. First reflection of reference beam, 6. Third reflection of reference beam, 7. Reflection of object beam

COHERENCE PEAK SENSING MICROSCOPE II

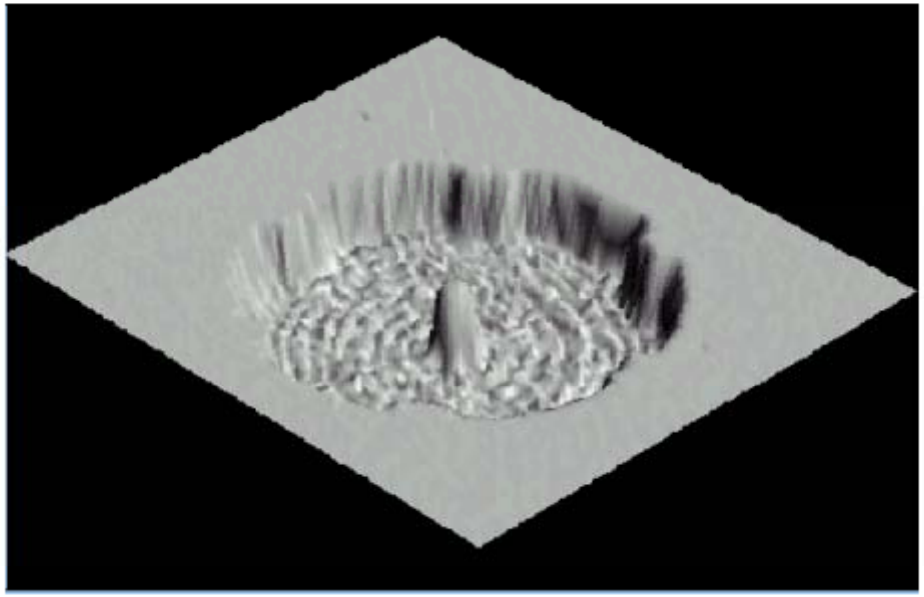

Figure 8. Results obtained using a vertical scanning coherence peak sensing measurement of a micro-machined silicon part. For this example the RMS of the surface is 2.3 microns and the P-V is 6.16 microns

Misure con ampia dinamica verticale (quella laterale dipende dall'ingrandimento del microscopio)

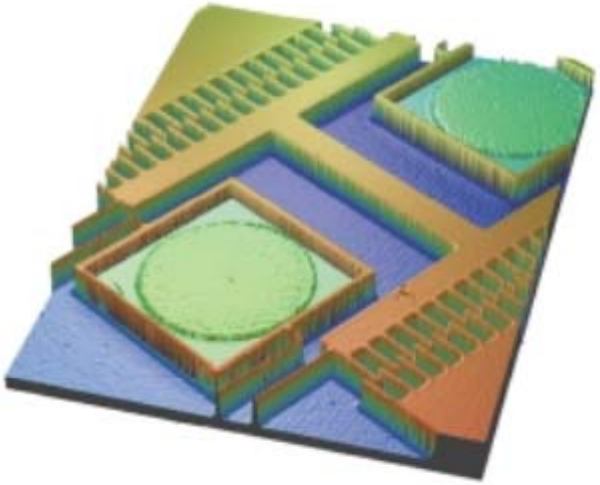

Figure 2. Example of MEMS structure – section of a comb capacitor drive measured using EVSI. High lateral and vertical resolution are combined with a large field of view. 950µm x 1.3mm

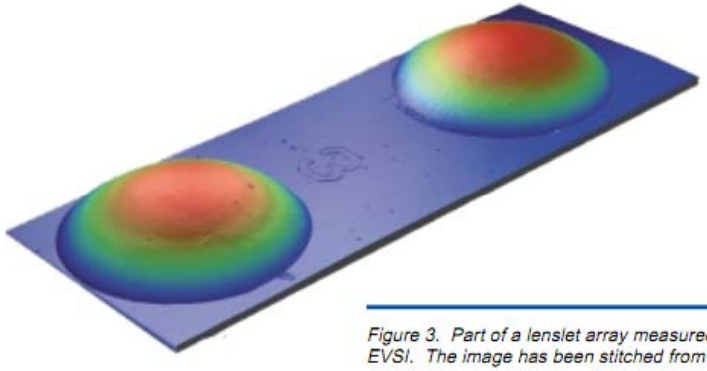

Figure 3. Part of a lenslet array measured using EVSI. The image has been stitched from two individual measurements. Each lenslet can be analyzed separately, as can its relative position in the array. 1.6mm x 620µm.

PROFILOMETRIA OTTICA

Estensione tecniche interferometriche al caso 2D: profilometria ottica (senza contatto)

Non-contact profilometers [edit]

An optical profilometer is a non-contact method for providing much of the same information as a stylus based profilometer. There are many different techniques which are currently being employed, such as laser triangulation (triangulation sensor), confocal microscopy and digital holography.

Advantages of optical profilometers

- Speed: Because the non-contact profilometer does not touch the surface the scan speeds are dictated by the light reflected from the surface and the speed of the acquisition electronics.
- Reliability: optical profilometers do not touch the surface and therefore cannot be damaged by surface wear or careless operators. Many non-contact Profilometers are solid-state which tends to reduce the required maintenance significantly.
- Spot size: The spot size, or lateral resolution, of optical methods ranges from a few micrometres down to sub micrometre.

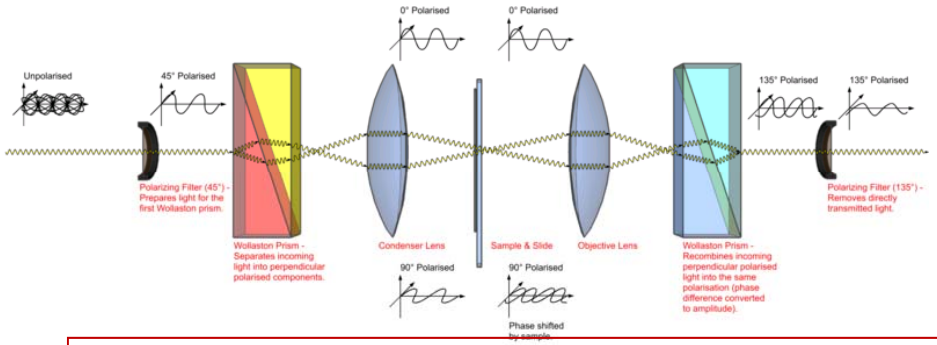

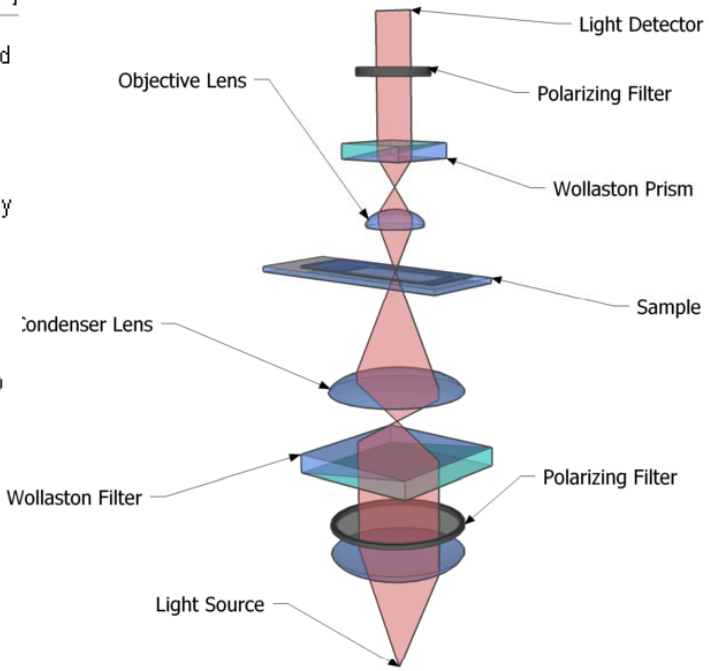

Microscopio Nomarski

Molte diverse configurazioni possibili e impiegate industrialmente

Un laser, un laser con due frequenze, due o più laser, sorgenti bianche (lampade)…

Sempre necessario avere due fasci con cammino ottico diverso che fanno interferenza

OLOGRAFIA

Holography is a technique which enables a light field, which is generally the product of a light source scattering off objects, to be recorded and later reconstructed when the original light field is no longer present (due to the absence of the original objects).[17] Holography can be thought of as somewhat similar to sound recording, whereby a sound field created by vibrating matter, like musical instruments or vocal chords, is encoded in such a way that it can be reproduced later without the presence of the original vibrating matter.

Holograms are recorded using a flash of light that illuminates a scene and then imprints on a recording medium, much in the way a photograph is recorded. A hologram, however, requires a laser as the light source, since lasers can be precisely controlled and have a fixed wavelength, unlike white light, which contains many different wavelengths.

Dennis Gabor
(06/05/1900 – 07/09/1979)
Hungarian scientist (invented the hologram)

A shutter is required when taking a photograph to limit the time in which the film is exposed to light. Holography also requires a specific exposure time, and this can be done using a shutter, or by electronic timing of the laser.

This laser beam is generally aimed through a series of elements that change it in different ways - see Figure 2. The first element is a beam splitter, which divides the beam into two identical beams, each aimed in different directions:

- One beam, known as the illumination or object beam, is spread using lenses and directed onto the scene using mirrors, in order to illuminate it. Some of the light scattered (reflected) from this illumination falls onto the recording medium.
- The second beam, known as the reference beam, is also spread through the use of lenses, but is directed so that it doesn't come in contact with the scene, and instead travels directly onto the recording medium.

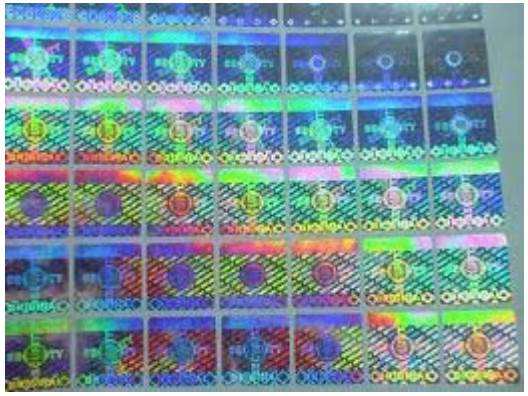

OLOGRAMMI PER “REGISTRARE” UN’IMMAGINE

http://www.xmx.it/ologrammi.htm

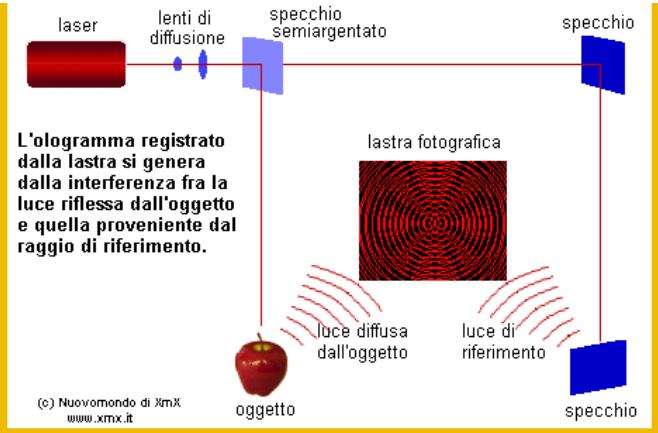

Qui sopra vediamo come si realizza l'ologramma. Un fascio di luce laser viene sdoppiato: una parte è inviata direttamente sulla lastra, mentre l'altra parte del fascio è diffusa dall'oggetto, prima di cadere sulla lastra. Nel percorrere tragitti diversi, le due componenti del fascio si sfasano l'una rispetto all'altra e, ricongiungendosi, producono una *figura di interferenza* che viene registrata sulla pellicola sotto forma di ologramma. Ad occhio nudo sulla lastra non è visibile alcuna immagine, solo una retinatura di linee sottilissime e iridescenti.

Registrazione

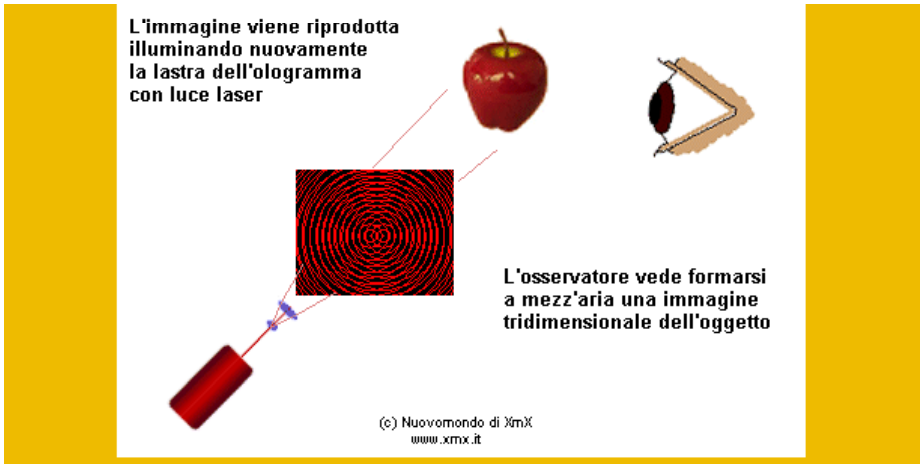

...qui sopra, per riprodurre l'ologramma lo osserviamo con la luce laser, proiettandone un fascio sulla lastra. Apparentemente a mezz'aria l'osservatore vede formarsi l'immagine tridimensionale, attorno alla quale si può anche girare per osservarla da tutti i punti di vista, proprio come se fosse un oggetto reale.

Lettura

Su una stessa lastra possono essere registrati moltissimi diversi ologrammi, semplicemente variando l'angolo di incidenza del laser, e allo stesso modo essi possono essere letti separatamente.

...infine qua sopra vediamo che l'informazione registrata (in questo caso l'immagine della mela) è distribuita su tutta la lastra. Infatti da ogni sua più piccola parte è possibile riavere l'informazione originale, anche se in tal caso si verifica una certa perdita d'informazione, inversamente proporzionale alla grandezza della parte letta.

“IMMAGINI” 3D

Holography is "lensless photography" in which an image is captured not as an image focused on film, but as an interference pattern at the film. Typically, coherent light from a laser is reflected from an object and combined at the film with light from a reference beam. This recorded interference pattern actually contains much more information that a focused image, and enables the viewer to view a true three-dimensional image which exhibits parallax. That is, the image will change its appearance if you look at it from a different angle, just as if you were looking at a real 3D object. In the case of a transmission hologram, you look through the film and see the three dimensional image suspended in midair at a point which corresponds to the position of the real object which was photographed.

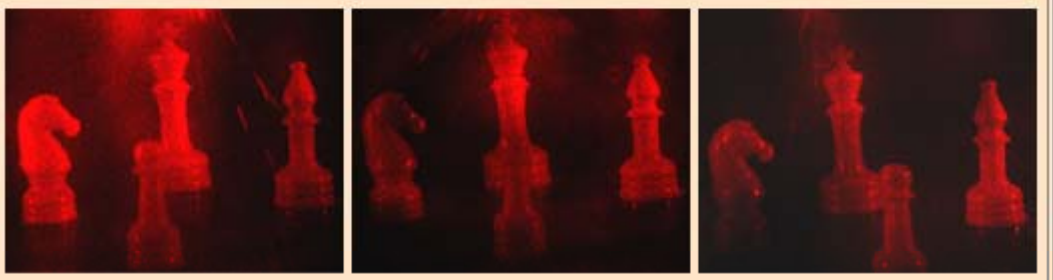

These three images of the same hologram were taken by positioning the camera at three positions, moving from left to right. Note that the pawn appears on the left side of the king in the left photo, but transitions to the right of the king as you sweep your eye across the hologram. This is real parallax, which tells you that the image is truly 3-dimensional. Each perspective corresponds to looking through the hologram at a particular point.

Nell’olografia è necessario avere un “buon” laser (grande lunghezza di coerenza) poiché le differenze di cammino ottico possono essere ampie

METROLOGIA OLOGRAFICA (CENNI) I

Multi-Wavelength digital holographic metrology

Carl C. Aleksoff
Coherix, Inc., 3980 Ranchero Drive, Ann Arbor, MI 48108

One of the most useful outgrowths of Emmett Leith's holographic work is its use in metrology[1]. The measurement of parts via holographic techniques started early at the Willow Run Labs of the University of Michigan with object deformation interferometry[2, 3], shape contouring[4] , and vibration analysis[5, 6]. In this paper we will consider a more modern outgrowth of using multi-wavelength digital holography to generate 3D (three dimensional) computer-based precision imagery of manufactured parts. These digital holographic techniques have been incorporated into the Coherix Shapix™ systems*, for which Emmett Leith was a consultant.

The output digital image is a 2D array of numbers, where each number represents a height *H* from a reference plane for a pixel. This data can be processed to generate various views on a monitor or mined for features such a deviation from specified shape or surface roughness.

The basic multi-wavelength measurement concept can be described from the standpoint of synthetic-aperture laser-radars[7, 8] or via interferometers[9]. In this paper will develop the basics of the process from an interferometric perspective because we are describing an image plane holographic system where each acquired image pixel can be described as part of a simple interferometer.

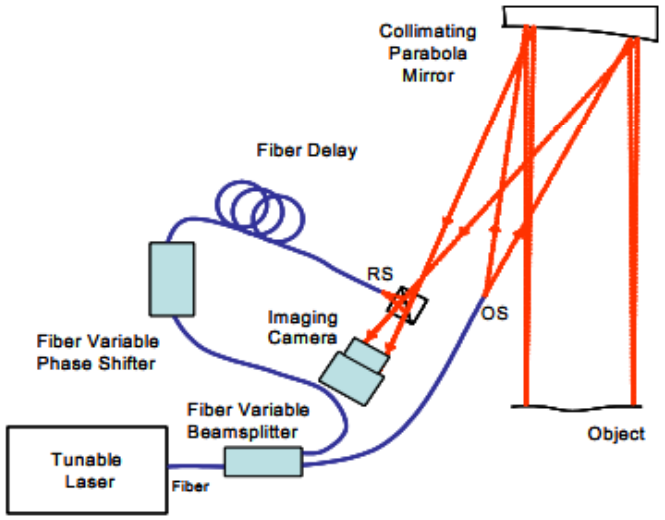

Fig. 1 The optical arrangement is shown for measuring the object height as a function lateral position illumination source (OS) is the end of one fiber and the reference source (RS) is at the other end reference source is at the same apparent position and distance from the camera as the focus of light v parabola from the object. The camera images the object as well as accepting a coaxial reference wav interference via the cube beamsplitter.

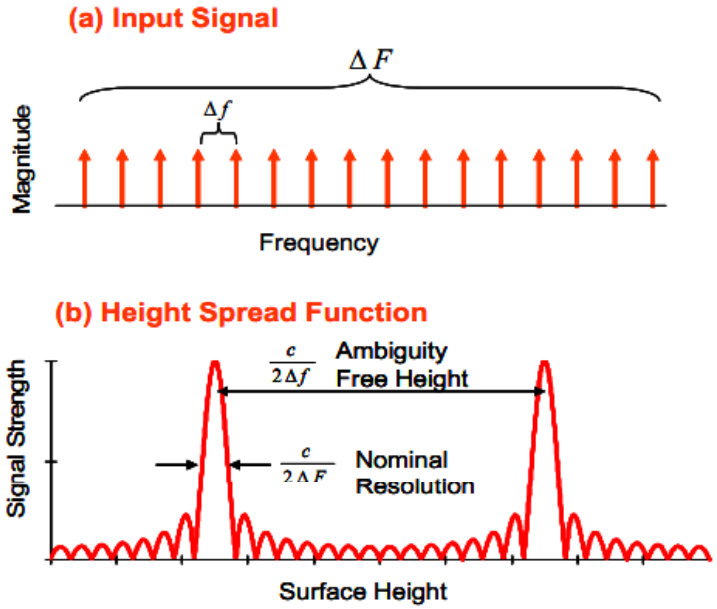

Fig. 3. These diagrams show the basic relationships the input and output data. The input data is a set of delta functions with the frequency spacing of the measurement frequencies (assumed equal spacing) and measured phases. The output is the magnitude of the Fourier Transform of the input data. The calculated surface height is at the first peak of the output.

SPECKLES (O SPECKLE PATTERNS)

A **speckle pattern** is a random intensity pattern produced by the mutual interference of a set of wavefronts.[1] This phenomenon has been investigated by scientists since the time of Newton, but speckles have come into prominence since the invention of the laser and have now found a variety of applications.

A familiar example is the random pattern created when a laser beam is scattered off a rough surface - see picture. A less familiar example of speckle is the highly magnified image of a star through imperfect optics or through the atmosphere (see speckle imaging). A speckle pattern can also be seen when sunlight is scattered by a fingernail.[2]

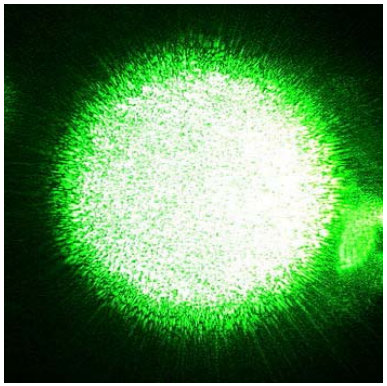

Gli speckles si osservano per esempio inviando la radiazione di un laser su una superficie non perfettamente levigata (e.g., un foglio di carta)

Essendo dovuto a interferenza, lo speckle ha caratteristiche ottiche “straordinarie” (e.g., è “sempre a fuoco”)

Electronic Speckle Pattern Interferometry (ESPI)[1], also known as TV Holography, is a technique which uses laser light, together with video detection, recording and processing to visualise static and dynamic displacements of components with optically rough surfaces. The visualisation is in the form of fringes on the image where each fringe normally represents a displacement of half a wavelength of the light used (i.e quarter of a micrometre or so).

ESPI can be used for stress and strain measurement, vibration mode analysis and nondestructive testing.

ESPI is similar to holographic interferometry in many ways, but there are also significant differences between the two techniques.

SPECKLE INTERFEROMETRY I

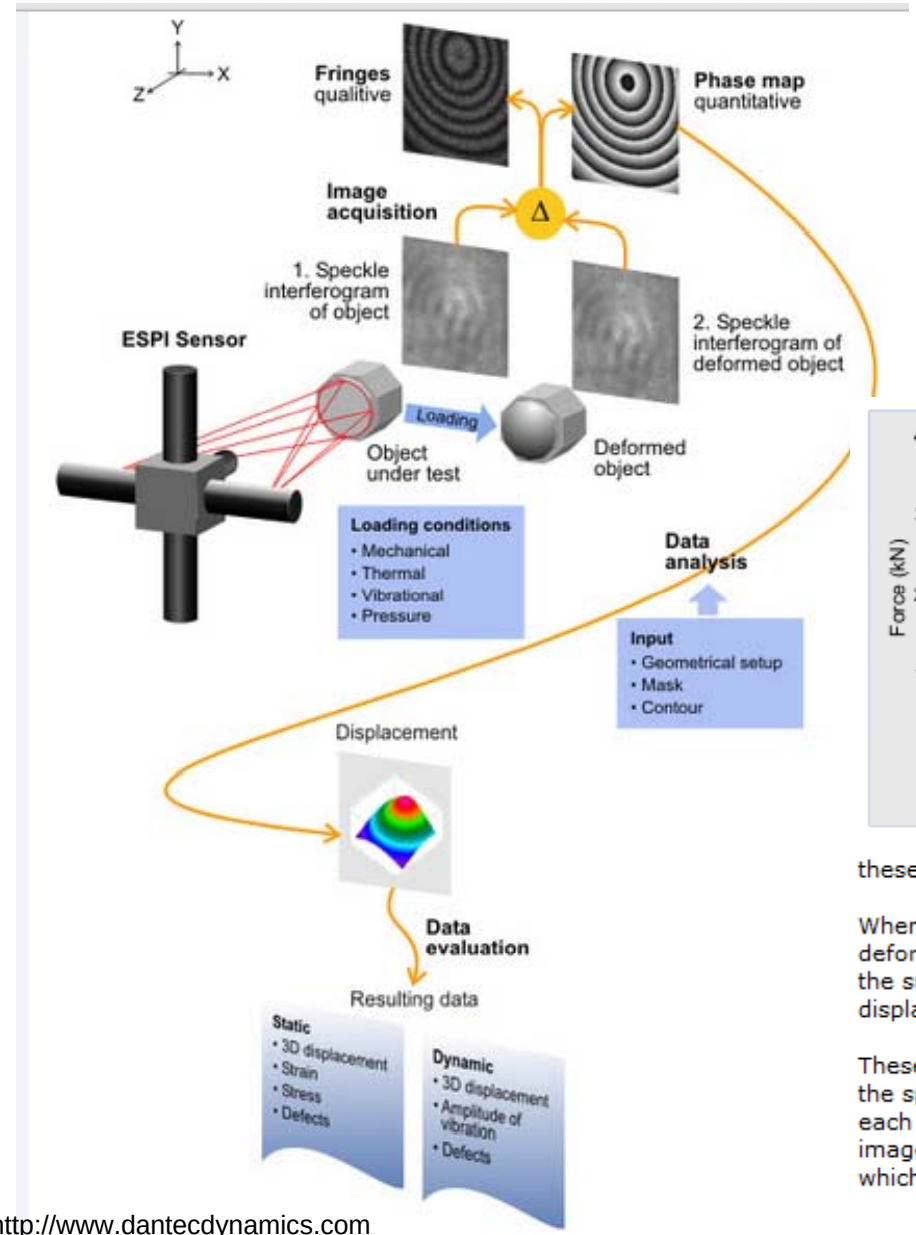

L'analisi delle frange di interferenza in real-time si usa per ricostruire la deformazione del provino in test di **stress-strain**

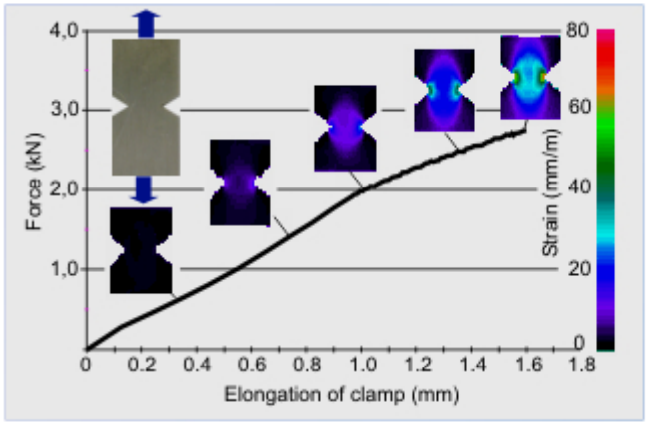

Principles
The illumination of a rough surface with coherent laser light and subsequent imaging using a CCD camera generates statistical interference patterns, the so-called speckles.

Like a fingerprint, these speckles are inherent to the investigated surface. Superimposing a reference light, which is split out of the same laser source, on these speckles results in an interferogram.

When the object under test is loaded, e.g. by mecha-nical means, and the surface is deformed, the speckle interferogram also changes. Comparing an interfero-gram of the surface before and after loading will result in a fringe pattern, which reveals the displacement of the surface during loading as contour lines of deformation.

These qualitative fringe images are of low contrast and noisy due to the presence of the speckles. A procedure called phase shifting takes a series of speckle images for each surface state and calculates a quantitative phase map. In contrast to the fringe images this phase map furthermore contains quantitative and directional information which can directly be transformed into a displacement value.

http://www.dantecdynamics.com

SPECKLE INTERFEROMETRY II

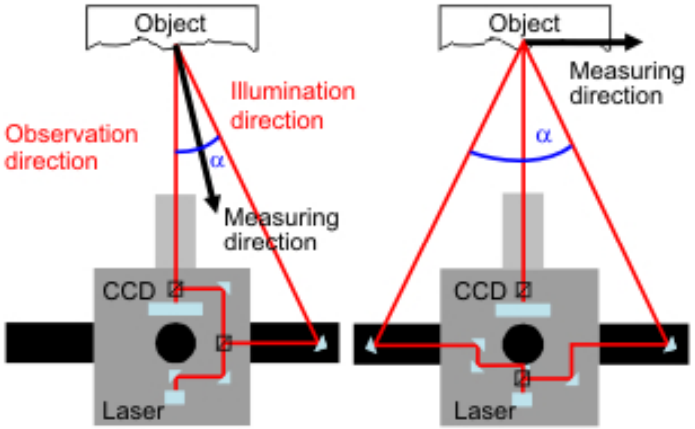

ESPI setup for out-of-plane measurement

$$d = \frac{N \cdot \lambda}{1 + \cos(\alpha / 2)}$$

ESPI setup for in-plane measurement

$$d = \frac{N \cdot \lambda}{2 \cdot \sin(\alpha / 2)}$$

d = displacement, N = number of fringes
λ = wavelength, α = illumination angle

3D information
In order to measure all three displacement components u, v and w, measurements should be performed in x, y and z directions. The z component of displacement is measured in an out-of-plane configuration, the x and y components in an in-plane arrangement. Modern sensors integrate all arrangements and allow one to toggle in milliseconds.

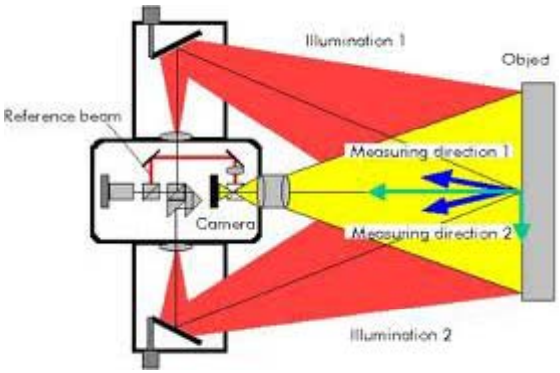

For static tests the three displacement directions are measured in series. In dynamic applications however, all sensitivity directions are acquired in parallel.

The resolution of the displacement is determined by the wavelength of the laser employed and the geome-trical arrangement. Typical values are down to 50 nm.

Strain/stress
The strain within the object due to a mechanical or thermal loading is calculated from the three dimensional displacement field. Therefore for nonplanar objects the contour is also measured. With known material parameters (Young's modulus, Poisson's ratio) the corresponding stress components in the linear elastic region are calculated from the strain components.

Applications
The full-field nature of the results allows an accurate and easy determination of material parameters and the iden-tification of highly stressed areas. In contrast to conven-tional methods e.g. strain gauge, scanning vibrometer, ESPI systems combine an unsurpassed density of measuring points with very high sensitivity and a dynamic range up to several hundred kHz.

Typical applications utilize not just a single measurement but a sequence of measurements, so that the user can follow the evolution of displacement/strain during loading.

METROLOGIA OLOGRAFICA (CENNI) II

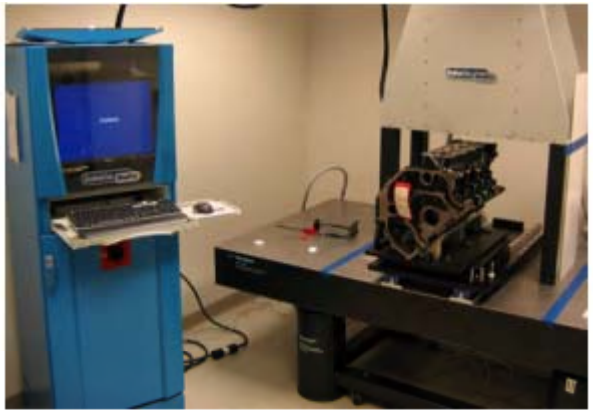

Fig.4. The Shapix system with an engine block inserted for measurement.

Fig. 5. A picture of the engine showing the cylinder deck face to be measured for flatness

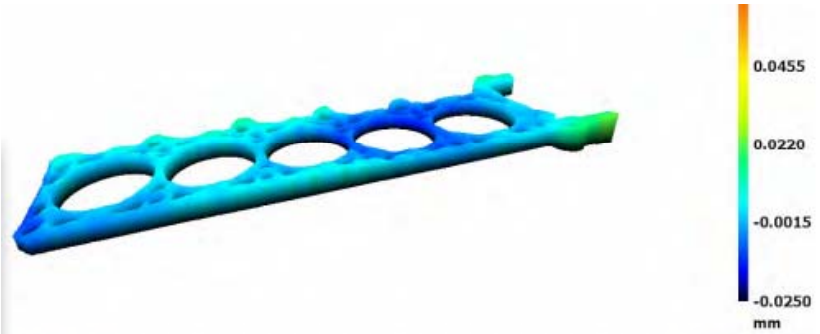

Fig. 6a A Shapix measured engine cylinder deck is shown as a 3D perspective image. This deck was cut with a new tool bit.

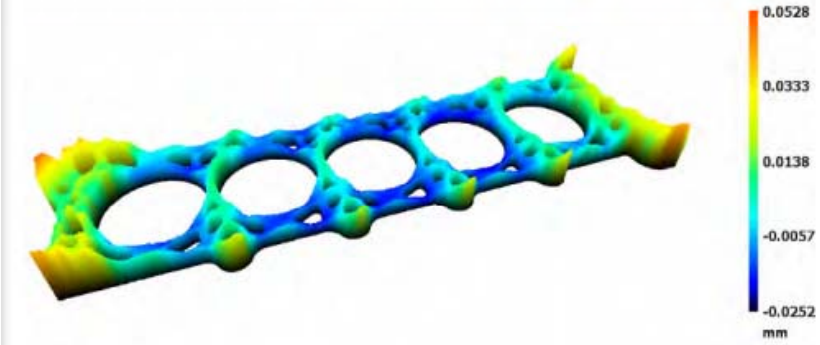

Fig. 6b. A Shapix measured engine cylinder deck is shown as a 3D perspective image. This deck was the 1800 unit cut with the tool bit.

Misure verticali molto accurate su un'estensione laterale molto grande!

PLASMA

In physics and chemistry, **plasma** is a state of matter similar to gas in which a certain portion of the particles are ionized. Heating a gas may ionize its molecules or atoms (reduce or increase the number of electrons in them), thus turning it into a plasma, which contains charged particles: positive ions and negative electrons or ions.[1] Ionization can be induced by other means, such as strong electromagnetic field applied with a laser or microwave generator, and is accompanied by the dissociation of molecular bonds, if present.[2]

The presence of a non-negligible number of charge carriers makes the plasma electrically conductive so that it responds strongly to electromagnetic fields. Plasma, therefore, has properties quite unlike those of solids, liquids, or gases and is considered a distinct state of matter. Like gas, plasma does not have a definite shape or a definite volume unless enclosed in a container; unlike gas, under the influence of a magnetic field, it may form structures such as filaments, beams and double layer. Some common plasmas are stars and neon signs. In the universe, plasma is the most common state of matter for ordinary matter, most of which is in the rarefied intergalactic plasma (particularly intracluster medium) and in stars.

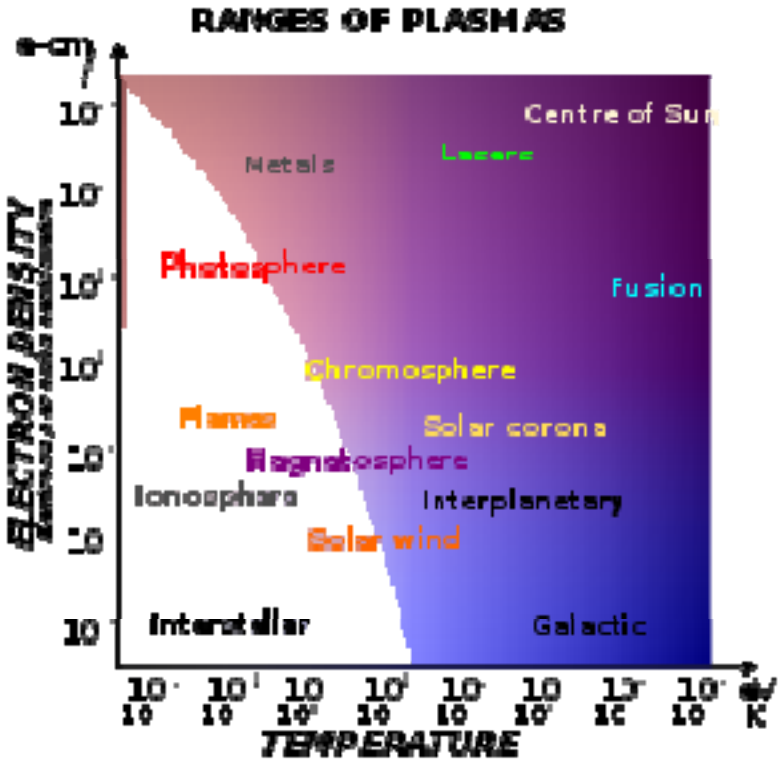

A plasma is very similar to a gaseous medium, expect that the electrons are *free*: *i.e.*, there is no restoring force due to nearby atomic nuclii. Hence, we can obtain an expression for the dielectric constant of a plasma from Eq. (1149) by setting ω_0 to zero, and n to the number density of electrons, n_e. We obtain

$$\epsilon = 1 - \frac{\omega_p^2}{\omega^2}, \tag{1150}$$

L'indice di rifrazione di un plasma dipende dalla sua densità

where the characteristic frequency

$$\omega_p = \sqrt{\frac{n_e\, e^2}{\epsilon_0\, m_e}} \tag{1151}$$

is called the *plasma frequency*. We can immediately see that formula (1150) is problematic. For frequencies above the plasma frequency, the dielectric constant of a plasma is less than unity. Hence, the refractive index $n = \sqrt{\epsilon}$ is also less than unity. This

SHADOWGRAPHY OF PLASMAS I

Measurement of the variation of refractive index allows the determination of several properties of a transparent medium. There are two different ways to obtain that variation: by beam-deflection angle measurement (shadowgraphy) or by phase measurement (interferometry). The shadowgraph technique consists of passing a pencil of light through the test section and letting it fall directly, or via an imaging lens, onto a recording device such as a photographic plate or a charged coupled device (CCD) matrix. In interferometry, the beam of light traversing the medium undergoes phase variations that can be revealed by interferometric methods.

In an interferometer, two beams travel along separate paths before they are recombined. This requirement has led to the development of a number of interferometers for specific

La variazione di indice di rifrazione produce una deflessione del fascio (cfr. dispersione da un prisma)

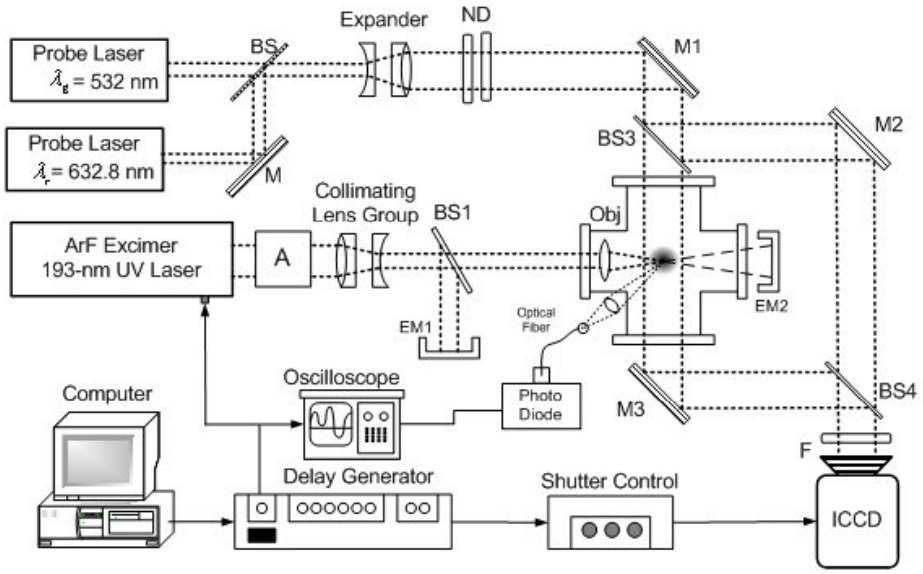

SHADOWGRAPHY OF PLASMAS II

Nel caso di plasmi transienti, e.g. creati mediante ablazione laser impulsata, gli shadowgrams (fatti a istanti diversi) mostrano l'evoluzione spazio-temporale del plasma

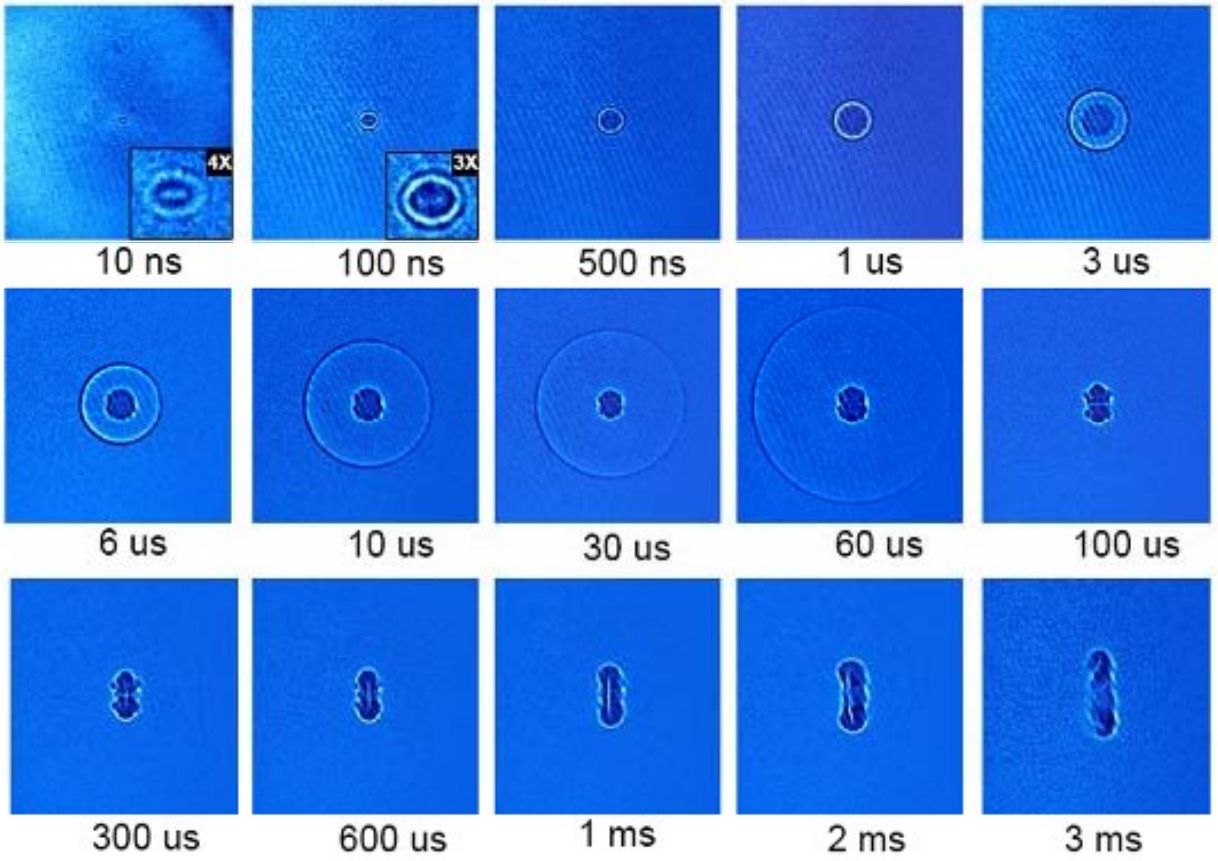

Shadowgrams of the 193 nm laser focused plasma in air, with laser input radiation of 135 mJ energy. Each image has a spatial extent of 2.5 cm. Gating time for each image is 10 ns.

SCHLIEREN SHADOWGRAPHY I

The optical setup of a Schlieren imaging system may comprise the following main sections: Parallel beam, focusing element, stop (sharp edge) and a camera. The parallel beam may be achieved by a point-like light source (a laser focused into a pinhole is sometimes used) placed in the focal point of a collimating optical element (lens or mirror). The focusing element may be a lens or a mirror. The optical stop may be realized by a razor placed horizontally or vertically in the focal point of the focusing element, carefully positioned to block the light spot image on its edge. The camera is positioned behind the stop and may be equipped with a suitable lens.

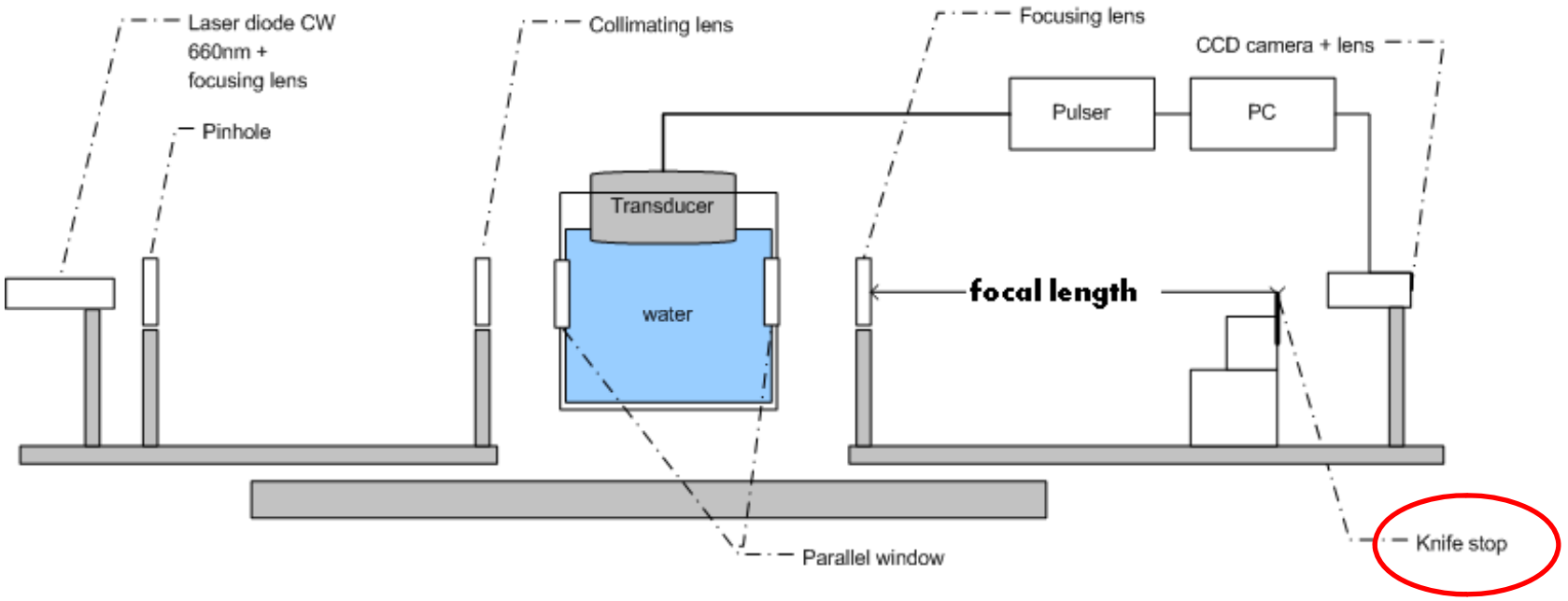

Si usa il bordo di una lama per selezionare spazialmente la radiazione che viene deflessa più o meno un certo angolo

SCHLIEREN SHADOWGRAPHY II

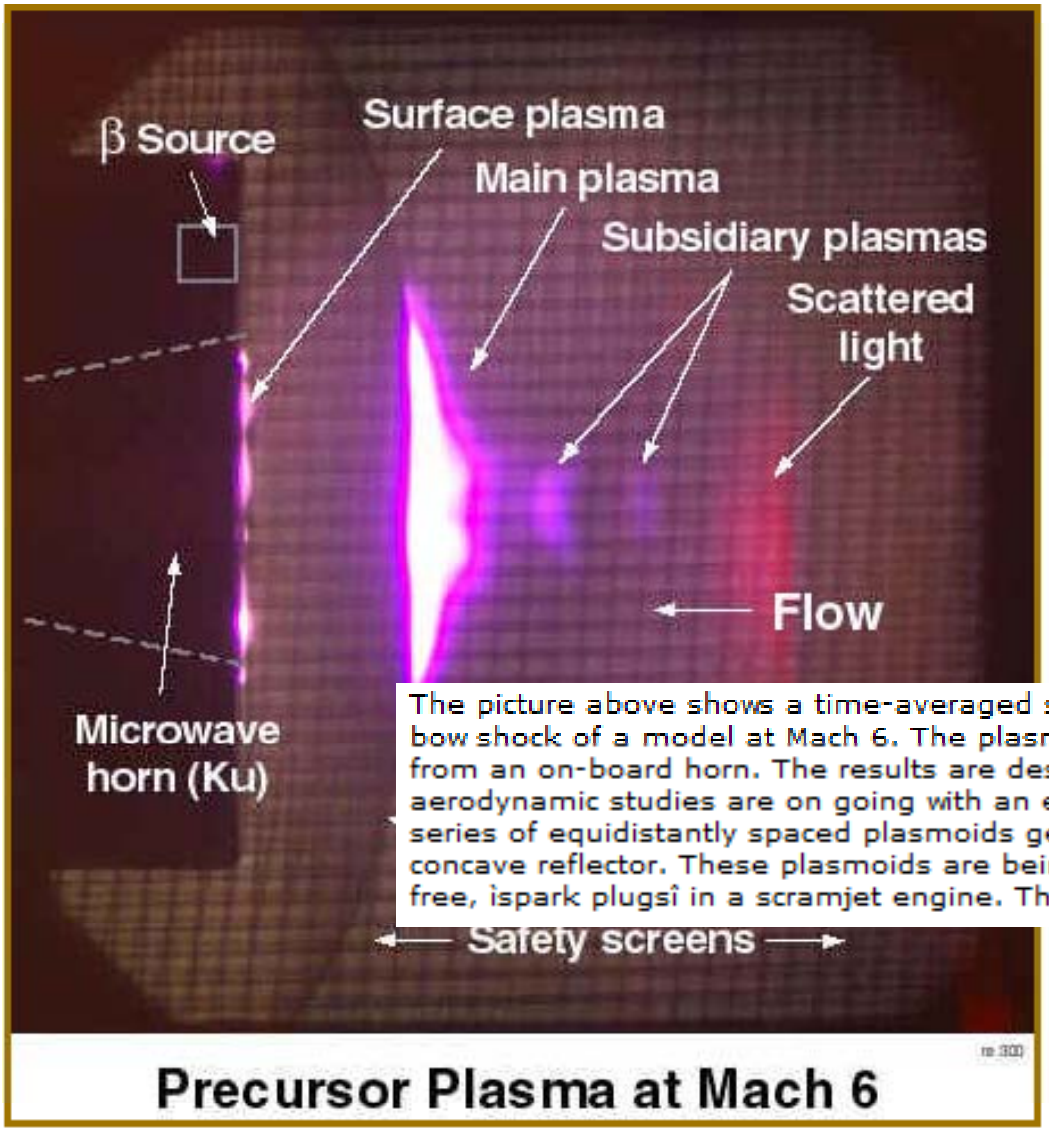

NATIONAL AERONAUTICS AND SPACE ADMINISTRATION

The picture above shows a time-averaged schlieren photograph of a precursor plasma situated on a bow shock of a model at Mach 6. The plasma was generated using high power, pulsed, microwaves from an on-board horn. The results are described in Phys. Plasmas, 8, 5013 (2001). These aerodynamic studies are on going with an emphasis on flow control. The figure below shows a series of equidistantly spaced plasmoids generated using a cavity formed by the horn and a concave reflector. These plasmoids are being studied for their possible use as freestanding, drag-free, ìspark plugsî in a scramjet engine. This volumetric plasma is described in AIAA-2003-4181.

SCHLIEREN SHADOWGRAPHY III

IOP Publishing — Journal of Physics D: Applied Physics
J. Phys. D: Appl. Phys. 44 (2011) 485202 (10pp) — doi:10.1088/0022-3727/44/48/485202

Quantitative shadowgraphy on a laminar argon plasma jet at atmospheric pressure

Grégoire de Izarra, Nuno Cerqueira and Charles de Izarra

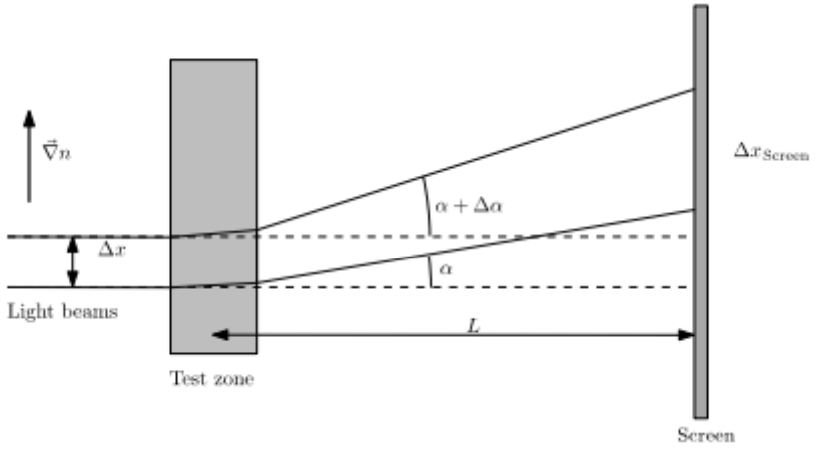

Figure 10. Principle of a shadowgraphy mounting.

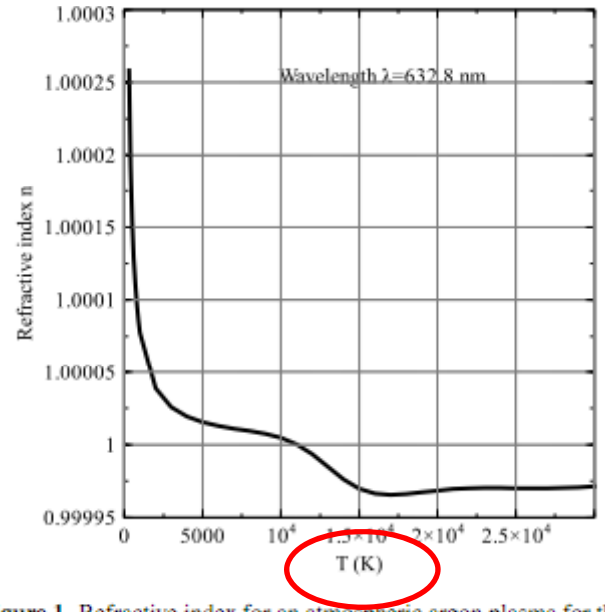

Figure 1. Refractive index for an atmospheric argon plasma for the wavelength $\lambda = 632.8$ nm.

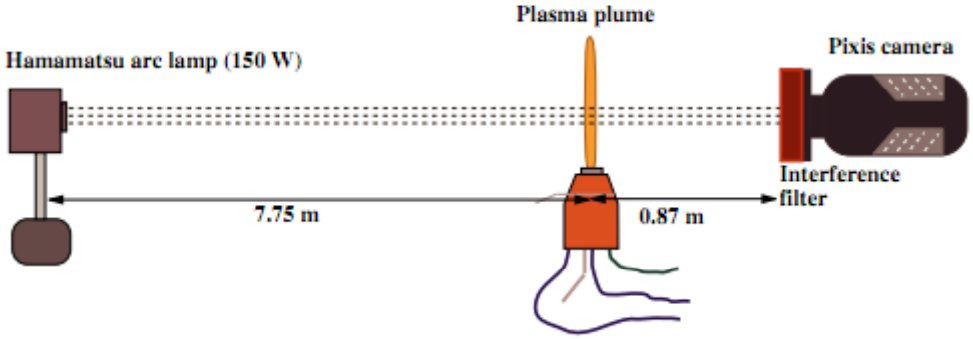

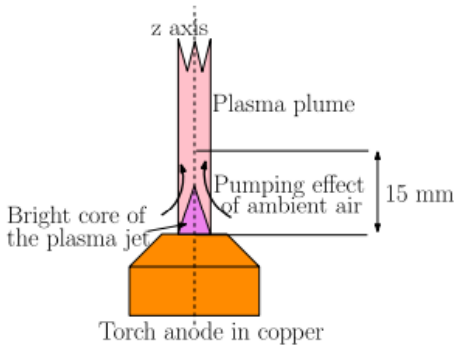

Figure 3. Pumping effect of the laminar plasma jet in air.

Per shadowgrams si può usare anche luce non laser

SHADOWGRAPHY & INTERFEROMETRY

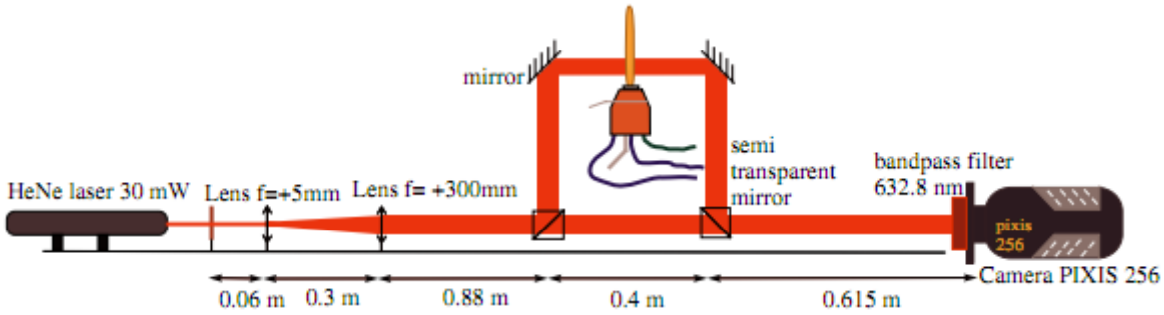

Figure 5. Mach–Zehnder interferometer.

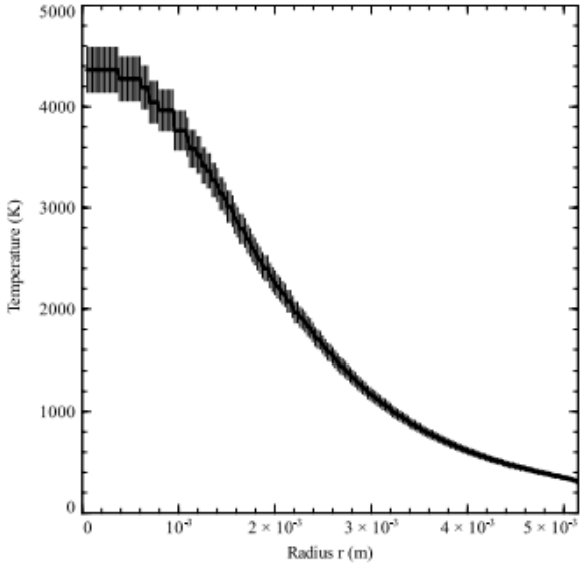

Figure 8. Temperature profile obtained using optical interferometry.

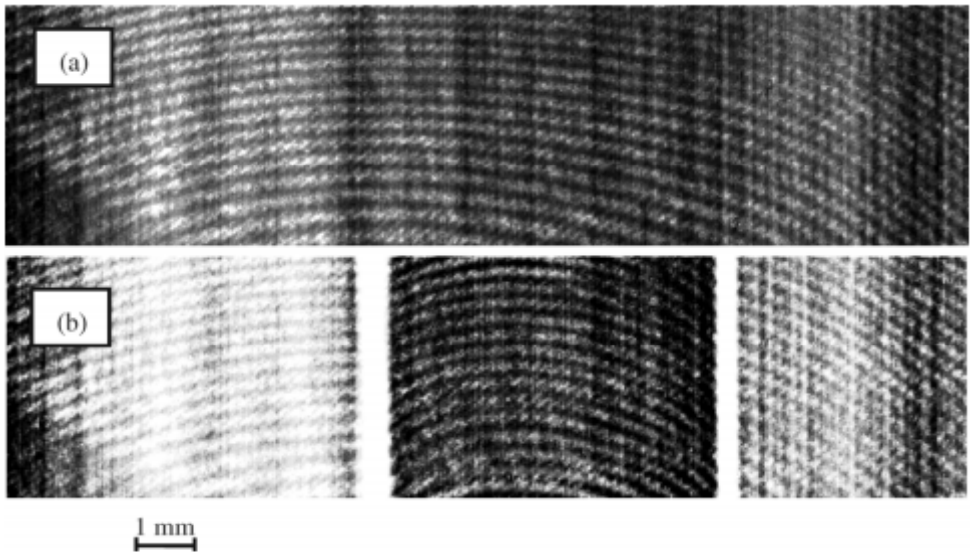

Figure 7. Interferograms: (*a*) reference (without plasma); (*b*) when the plasma is on.

Ma per risultati quantitativi meglio l'interferometria

INTERFEROMETRIA SU PLASMI I

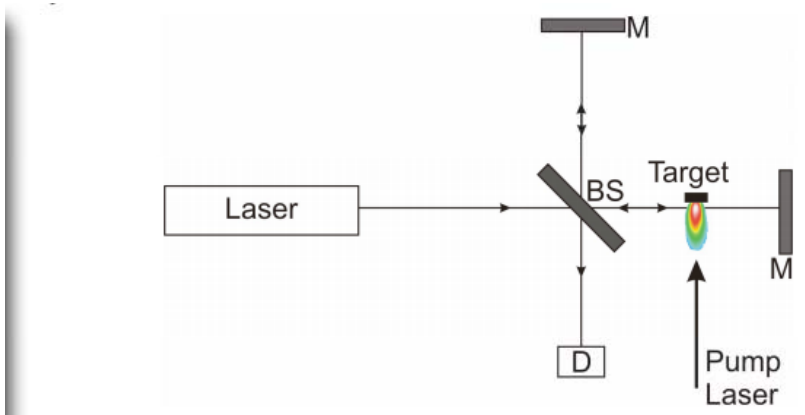

Fig. 1. Typical set-up for plasma density measurement using Michelson Interferome

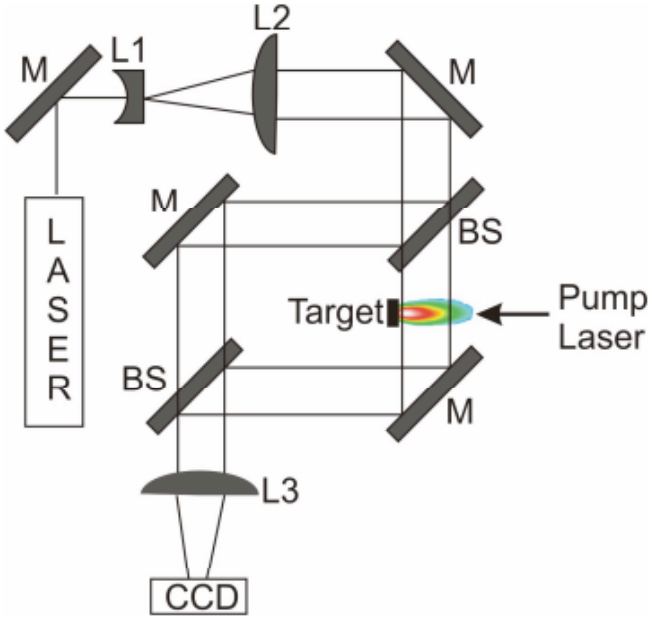

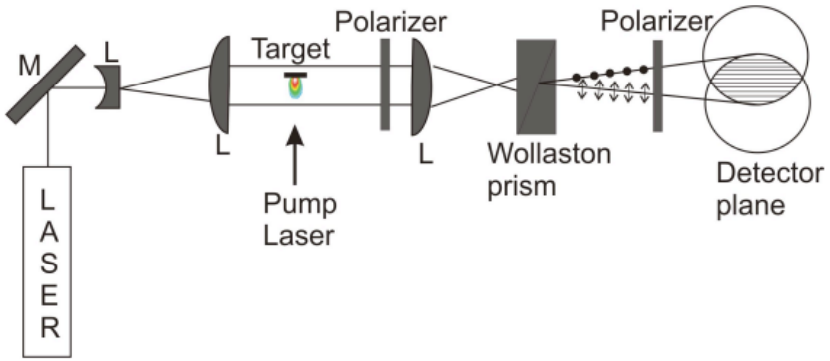

Fig. 3. Schematic of the Nomarski interferometer for measuring plasma densities. For better illustration the detector plane is shown tilted by 90 degrees.

. Mach-Zender interferometer set up for plasma density measurement.

Numerose configurazioni di interferometri possono essere utilizzate

INTERFEROMETRIA SU PLASMI II

plasma may consist of ions, atoms and molecules in addition to free electrons; the probe laser wavelength selected should be well away from any absorption resonances in the plume so that contributions to the refractive index from bound electrons is negligible compared to that of free electrons in the plasma. Then the refractive index (μ) can be expressed as

$$\mu = (1 - n_e/n_c)^{1/2} \qquad (1)$$

where n_e is the electron number density and n_c is the critical electron density corresponding to the probe laser wavelength λ ($n_c = 10^{21}\lambda^{-2}$ cm^{-3}, where λ is in microns). The probe laser radiation penetrates the plasma only to the point where the electron density reaches the critical density, at which point the reflection occurs. The ratio of the fringe shift to the fringe spacing (Δ) can be related to the line integral of electron density along the probe beam path by

$$\Delta = (2\lambda n_c)^{-1} \int n_e(l)\,dl \qquad (2)$$

where λ is the probe laser wavelength and l is the optical path length through the plume. A 2-dimensional mapping of the density can be obtained with the help of Abel inversion technique.

La radiazione penetra nel plasma “finché può”

Esiste quindi un efficiente meccanismo di contrasto per l’”immagine” creata

La densità del plasma può essere determinata localmente e con grande precisione

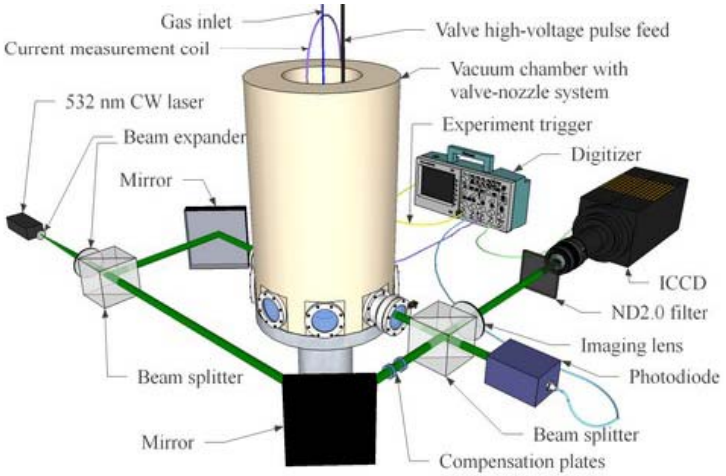

INTERFEROMETRIA SU PLASMI III

Shadowgrams (ps-resolved)

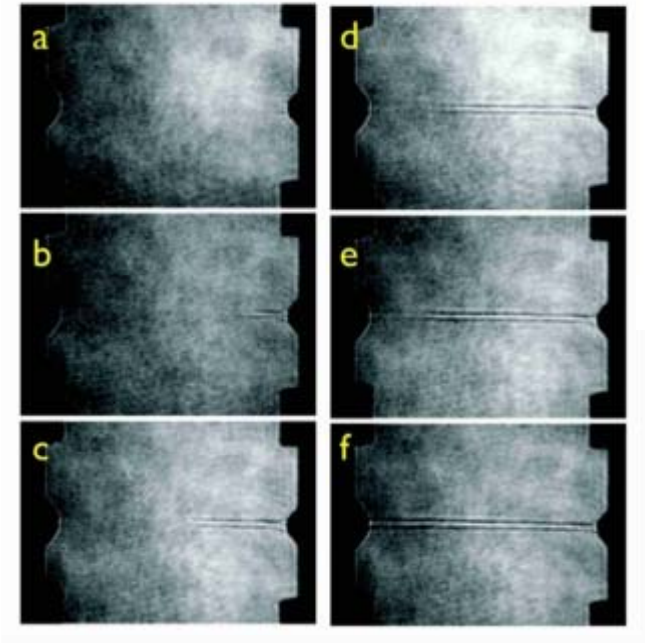

Plasma line evolution, sequence of pictures taken using transve
picosecond probe laser beam

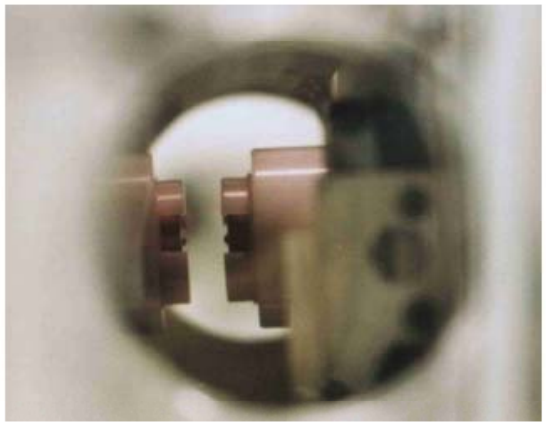

Elettrodi di scarica

Picture of conic shaped hollow electrodes inside the vacuum chamber

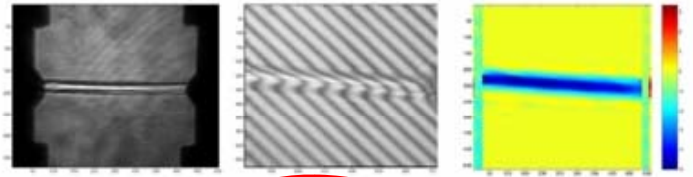

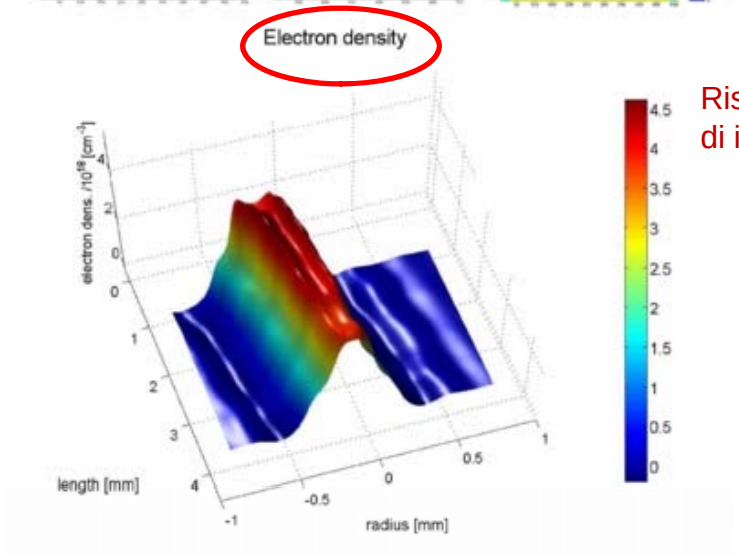

Risultati delle misure di interferometria

Shadowgraphy, partial view interferometry, interferogram phase and partial view of the plasma density, obtained using Abel inversion of the phase, of a plasma channel produced by a laser-triggered high-voltage discharge on a free space background of helium.

http://cfp.ist.utl.pt

DIAGNOSTICHE “ANALITICHE”

L’interazione radiazione/materia è tradizionalmente impiegata per scopi **spettroscopici**

Spettroscopia:
tecnica “analitica”, species-selective, (spesso) quantitativa, facilmente adattabile a misure risolte temporalmente e/o spazialmente

Richiede sorgenti sintonizzabili!!

Esempio:
Spettroscopia di fluorescenza (emissione)
Spettroscopia di assorbimento

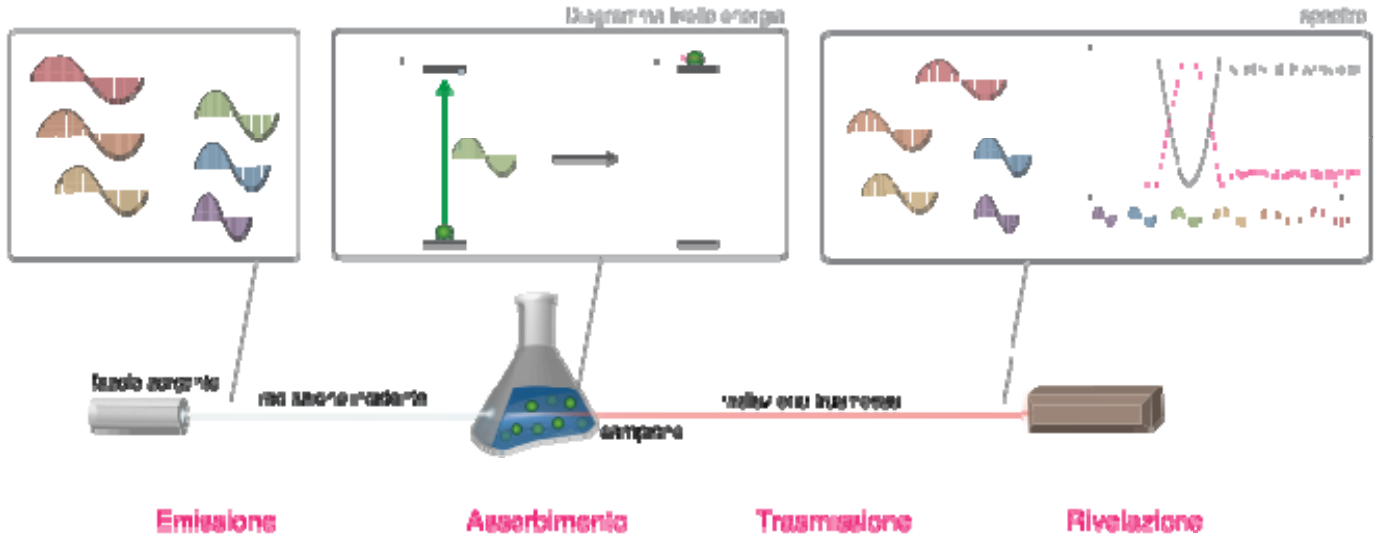

SINTONIZZABILITÀ

Lo spettro di guadagno del mezzo attivo ha normalmente larghezze “piccole” (typ. 1-10GHz)
→Eventuale sintonizzabilità è selezione dei modi (oppure scelta della riga attiva, e.g. Ar^+,CO_2)

Eccezioni: laser con mezzi attivi “a banda larga”:
-Laser a colorante (in soluzione o allo stato solido
-Laser a diodo (bande invece di livelli discreti…)

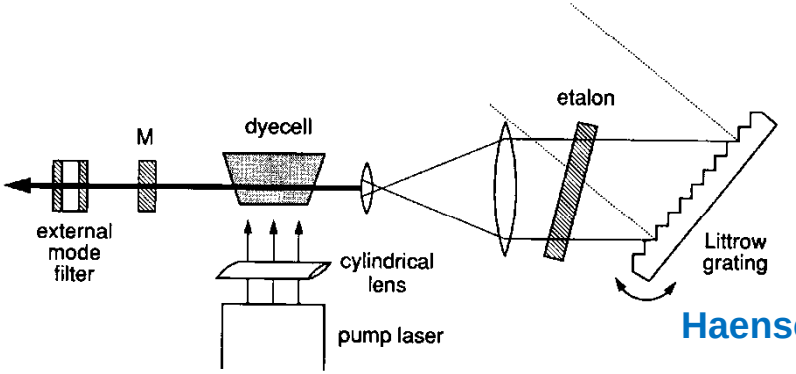

Haensch

Fig.5.44. Short Hänsch-type dye-laser cavity with Littrow grating and mode selection either with an internal etalon or an external FPI as "mode filter" [5.57]

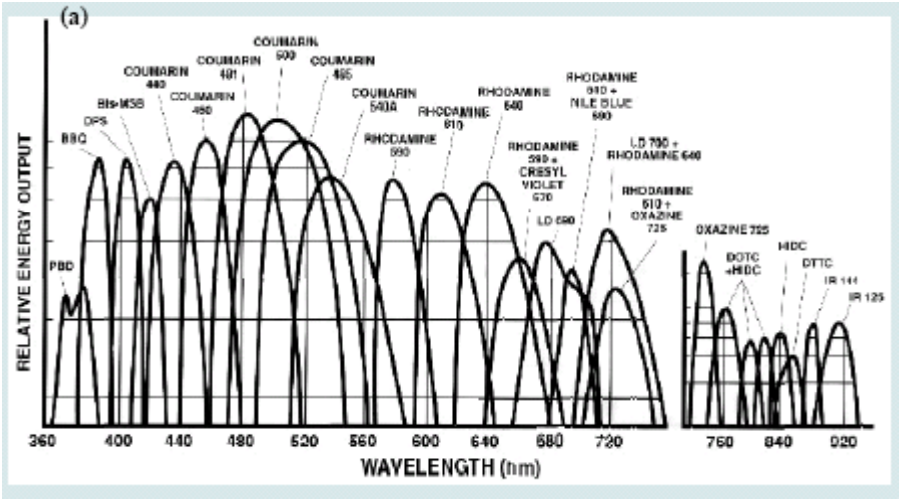

Cavità terminate da reticolo di diffrazione invece che specchi

When there is a need to separate light of different wavelengths with high resolution, then a diffraction grating is most often the tool of choice. This "super prism" aspect of the diffraction grating leads to application for measuring atomic spectra in both laboratory instruments and telescopes. A large number of parallel, closely spaced slits constitutes a diffraction grating. The condition for maximum intensity is the same as that for the double slit or multiple slits, but with a large number of slits the intensity maximum is very sharp and narrow, providing the high resolution for spectroscopic applications. The peak intensities are also much higher for the grating than for the double slit.

DIFFRACTION GRATINGS

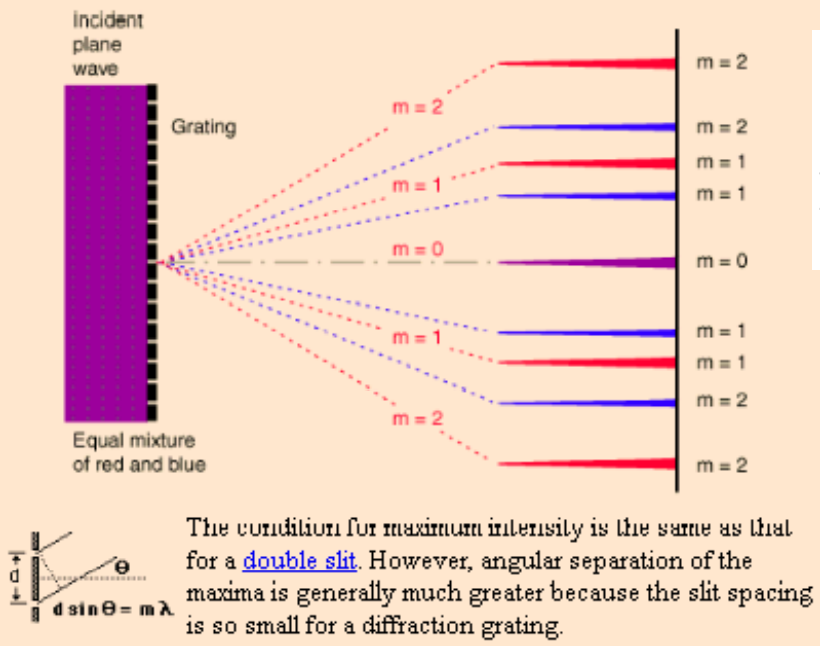

The condition for maximum intensity is the same as that for a double slit. However, angular separation of the maxima is generally much greater because the slit spacing is so small for a diffraction grating.

$$d \sin\theta_m = m\lambda.$$

Tipicamente d = *1/3600-1/600* mm^{-1}

It is straightforward to show that if a plane wave is incident at an angle θ_i, the grating equation becomes

$$d\,(\sin\theta_m + \sin\theta_i) = m\lambda.$$

The light that corresponds to direct transmission (or specular reflection in the case of a reflection grating) is called the zero order, and is denoted $m = 0$. The other maxima occur at angles which are represented by non-zero integers m. Note that m can be positive or negative, resulting in diffracted orders on both sides of the zero order beam.

La diffrazione dal reticolo segue le leggi dell'interferenza da sorgenti (slits) multiple

Riflessione massima ad una determinata combinazione di angoli di incidenza e riflessione

La cavità terminata da un reticolo ha perdite dipendenti dalla lunghezza d'onda

↓

Laser può operare solo se le perdite sono minori del guadagno

↓

Emissione sintonizzabile

FEEDBACK OTTICO IN DIODI LASER

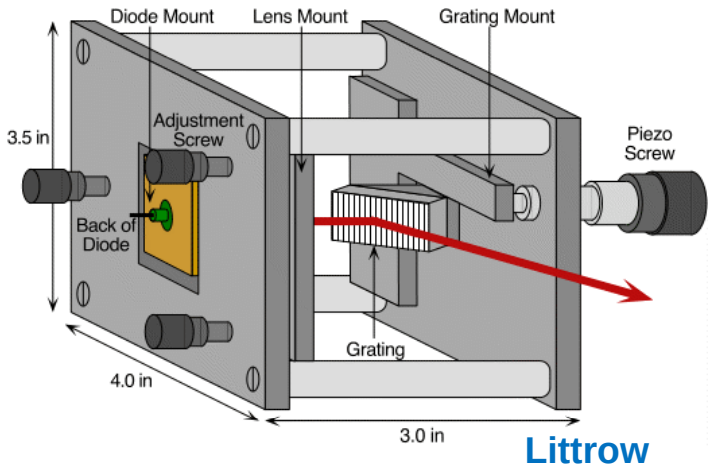

Littrow

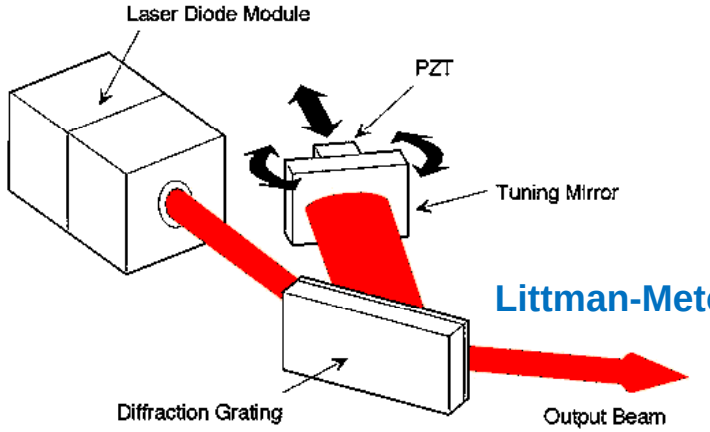

Littman-Metcalf

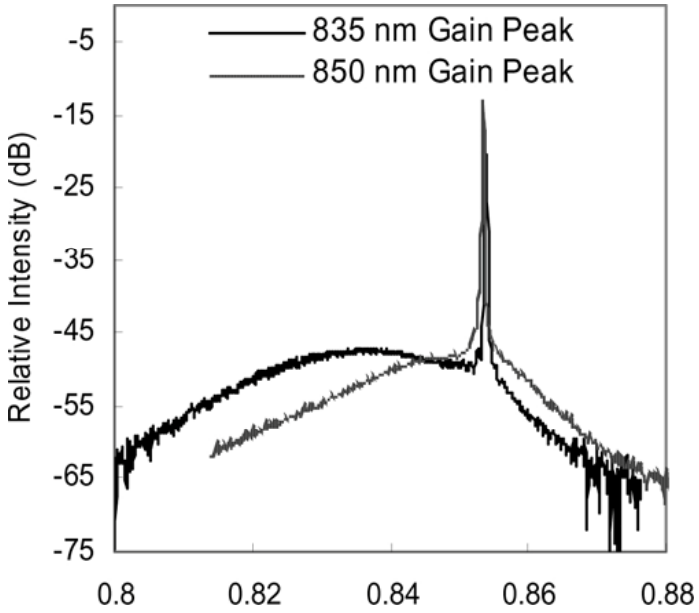

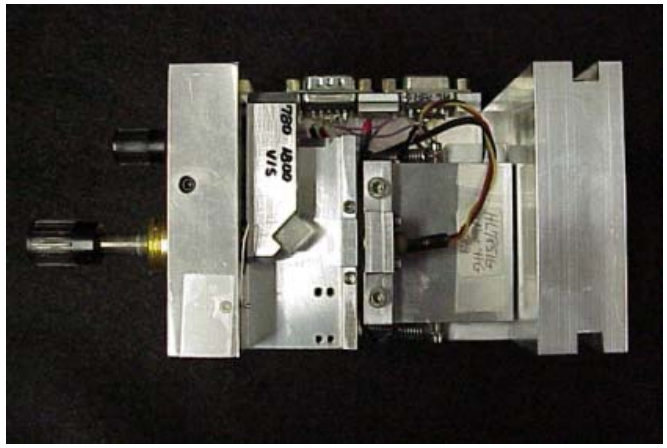

Due cavità accoppiate (interna, quella del laser, esterna, quella terminata da reticolo)
L'esterna ha free spectral range molto più basso e "costringe" il laser a emettere a una determinata frequenza dentro la riga di guadagno del materiale (molto larga)
La cavità esterna è sintonizzabile (e.g., reticolo attuato con PZT)

STABILIZZAZIONE LASER

Laser possono essere stabilizzati rispetto a vari parametri (e.g., ampiezza, frequenza)

Strategia di stabilizzazione: feedback elettronico (PID) su riferimento → lunghezza cavità

- The optical frequency of a single-frequency laser, or the frequency of one line of the frequency comb from a mode-locked laser, can be stabilized via resonator length control. The feedback signal can be obtained e.g. by recording a beat note with a second laser, by measuring the transmission or reflection of a very stable reference cavity, or by measuring the transmission of some absorption cell (e.g. an iodine cell), possibly using Doppler-free spectroscopy. A frequently used technique for generating an error signal is the Pound-Drever-Hall method [2, 3], using a weak phase modulation of the light which is sent to a reference cavity. A scheme not requiring such modulation is the Hänsch-Couillaud method [1].

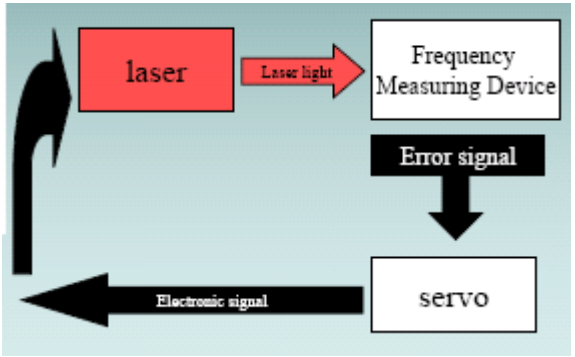

Cella di riferimento (assorbitore)

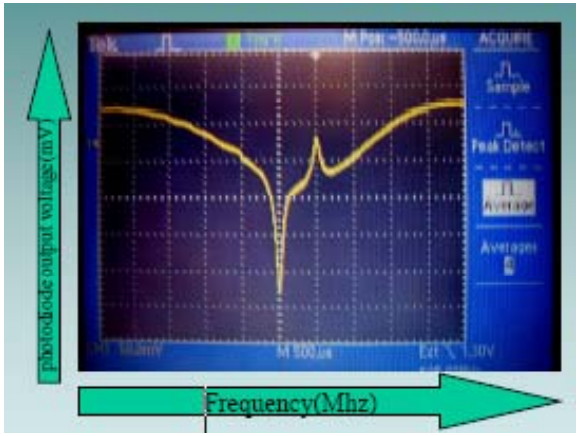

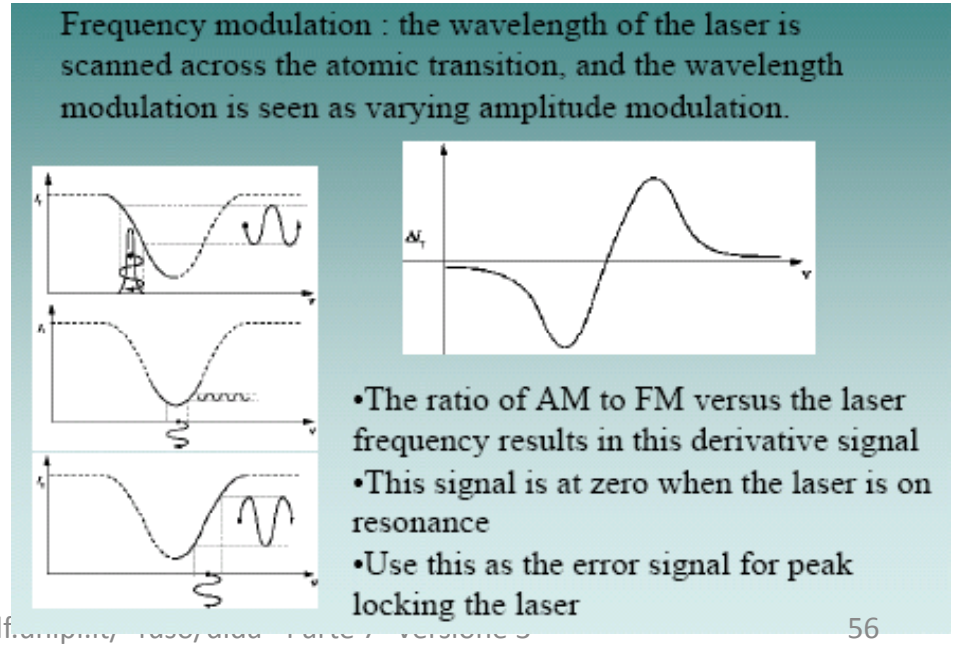

Tecniche di stabilizzazione più raffinate (e.g., Pound-Drever) per arrivare a stabilità 10^{-10} - 10^{-12} e larghezze di riga < 1Hz (su tempi brevi)

LASER-INDUCED FLUORESCENCE SU PLASMA

Laser induced fluorescence in a pulsed argon plasma

026107-2 Scime *et al.*

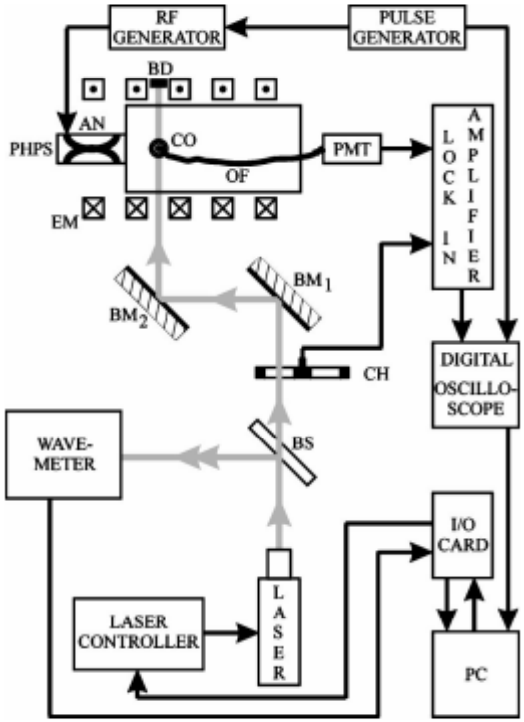

FIG. 1. Experimental setup for time resolved LIF diagnostic: PHPS - pulsed helicon plasma source, AN - antenna, EM - electromagnets, BD - beam dump, CO - collection optics, OF - optical fiber, PMT - photomultiplier tube, $BM_{1,2}$ alignment mirrors, CH - mechanical chopper, BS - beam splitter.

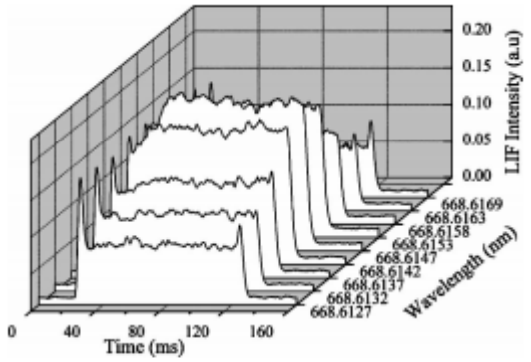

FIG. 2. A set of nine LIF signals averaged over 100 rf pulses without deconvolution. The data are separated by wavelength to highlight the difference in LIF signal as the laser is tuned through the absorption line.

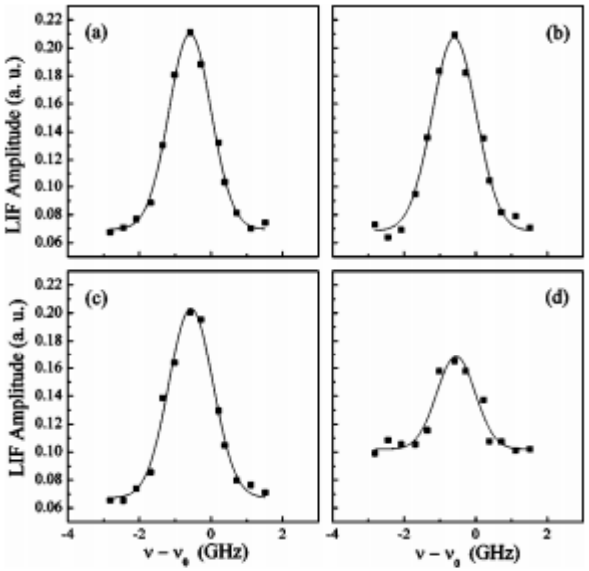

FIG. 4. Ion velocity distribution functions obtained from slices of the time dependent LIF signals during the pulse at: (a) t=50 ms; (b) t=75 ms; (c) t =100 ms; and (d) t=125 ms.

Misure selettive con risoluzione spaziale e temporale

ABSORPTION SPECTROSCOPY DA PLASMA

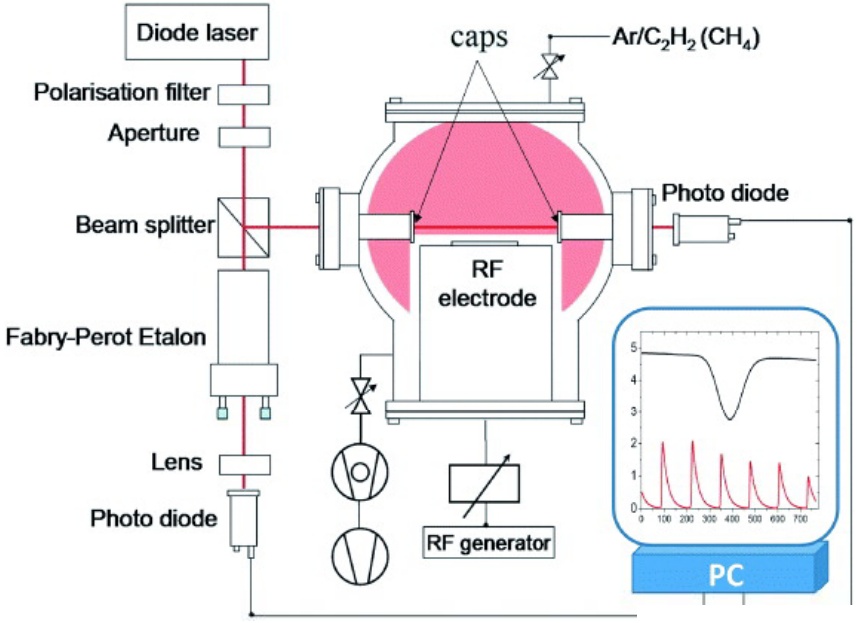

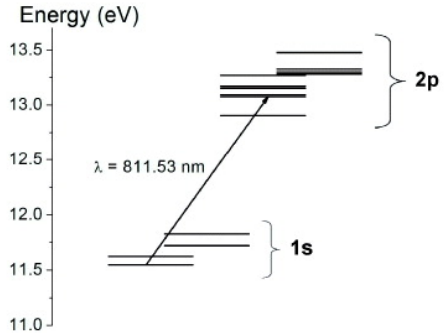

Argon

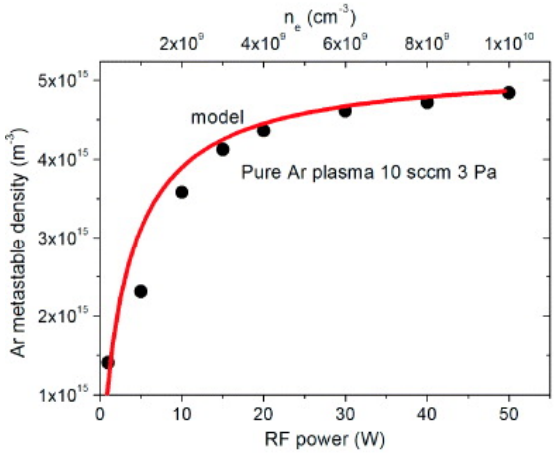

New J. Phys. **11** (2009) 033020
doi:10.1088/1367-2630/11/3/033020

Tunable diode laser absorption spectroscopy of argon metastable atoms in Ar/C_2H_2 dusty plasmas

Hoang Tung Do[1], Vladimir Sushkov and Rainer Hippler

The laser system consists of a tunable single-mode diode laser and a control unit for diode temperature and diode current (Toptica DL 100). The diode laser utilizes an extended cavity laser set-up with optical feedback into the laser diode from the first order of a spectrally selective grating. The laser light traverses a polarization filter and is directed to a beam splitter. The transmitted light is registered by a photo diode behind a Fabry–Perot etalon to monitor the light frequency [17]. The second light beam traverses the plasma chamber and is detected by a second photodiode.

Without plasma, the laser intensity, as measured by the second photodiode, linearly increases. In the case of a burning discharge, the photodiode signal shows pronounced variations in the neighborhood of a wavelength of 811.53 nm due to absorption by excited argon atoms (see figure 2). The transmitted intensity follows the Lambert–Beer law of absorption. Under the assumption of a constant Ar density inside the plasma region, and the Doppler broadening of the absorption line, the atom density n_m is related to the integrated absorption profile κ(ν) [26]

$$n_{\mathrm{m}} = \frac{4\pi\,\varepsilon_0 m_e c}{e_0^2 f \lambda_0}\sqrt{\frac{2kT}{\pi\, m_{\mathrm{a}}}}\kappa_0, \qquad (1)$$

where κ_0 is the absorption coefficient in the center of the profile, ε_0 is the dielectric constant, c is the speed of light, m_e and e_0 are the electron mass and charge, respectively, m_a is the atomic mass of Ar, k is the Boltzmann constant, λ_0 = 811.53 nm is the central wavelength of the investigated transition and f is the optical oscillator strength for the investigated transition. The width of the absorption signal is related to the temperature T of Ar atoms by the equation

$$T = \frac{\lambda_0^2 m_{\mathrm{a}}}{8k\ln 2}\Delta\nu^2, \qquad (2)$$

where Δν is the effective full-width at half-maximum of the measured absorption profile.

CONCLUSIONI

Le proprietà della luce laser sono ben interpretate sulla base del comportamento di:

- emissione stimolata
- guadagno del mezzo attivo (pompato)
- **cavità ottica risonante**

Esistono tecniche in grado di migliorare alcune caratteristiche della luce, in particolare quelle di larghezza di riga (monocromaticità) e quindi lunghezza di coerenza

L'elevata coerenza della luce laser è essenziale per applicazioni tecnologiche in metrologia, come: interferenza, profilometria, olografia, etc.

La monocromaticità e la possibilità di sintonizzazione di alcuni laser si offrono per l'impiego in diagnostiche, e.g., per plasmi